Modulation of fatty acid elongation generates sexually dimorphic hydrocarbons and female attractiveness in *Blattella germanica* (L.)

Xiao-Jin Pei [a], Yong-Liang Fan [a, *], Yu Bai [b], Tian-Tian Bai [a], Coby Schal [c], Zhan-Feng Zhang [a], Nan Chen [b], Sheng Li [b], and Tong-Xian Liu [a, *]

[a] State Key Laboratory of Crop Stress Biology for Arid Areas and Key Laboratory of Integrated Pest Management on Crops in Northwestern Loess Plateau, Ministry of Agriculture, Northwest A&F University, Yangling, Shaanxi 712100, P. R. China

[b] Guangdong Provincial Key Laboratory of Insect Developmental Biology and Applied Technology and Institute of Insect Science and Technology, School of Life Sciences, South China Normal University, Guangzhou 510631, China

[c] North Carolina State University, Department of Entomology and Plant Pathology and W.M. Keck Center for Behavioral Biology, Raleigh, North Carolina, USA.

* Corresponding authors:

Y.-L. Fan (yfan@nwafu.edu.cn) and T.-X. Liu (txliu@nwafu.edu.cn).

E-mail addresses:

X.-J. Pei: xiaojinpei@nwafu.edu.cn

Y.-L. Fan: yfan@nwafu.edu.cn

T.-X. Liu: txliu@nwafu.edu.cn

Abstract

Insect cuticular compounds serve multiple functions. As important intersexual signaling chemicals, they show variation between the sexes, but little is known about the underlying molecular mechanisms. Here, we report that sexually dimorphic hydrocarbons (SDHCs) are generated by a fatty acid elongase gene that is regulated by sex-differentiation genes in the German cockroach, *Blattella germanica*. Sexually mature females possess more C29 cuticular hydrocarbons (CHCs), especially the contact sex pheromone precursor 3,11-DimeC29. An RNAi screen and heterologous expression revealed that *BgElo12* and *BgElo24* were involved in HC production, but only *BgElo12* was responsible for SDHCs. Repressing female-enriched *BgElo12* masculinized the female CHC profile, decreased contact sex pheromone level, and reduced the female's sexual attractiveness. Moreover, RNAi of the sex-differentiation genes *BgTra* or *BgDsx* modulated both *BgElo12* transcripts and CHC profiles in females and males. The SDHCs are shaped by sexual selection, as females use them to keep high levels of sex pheromone.

Introduction

Sexual dimorphism is prevalent in the animal kingdom. Females and males independently evolve some traits that enhance survival and reproduction under the pressure of divergent selection forces, thus leading to sexual dimorphism of traits such as body size (Bear and Monteiro, 2013). Under sexual selection, asymmetric selection on the sexes can also result in the evolution of sexually dimorphism traits; however, these traits are subject to both inter- and intra-sexual selection (Darwin, 1871; Andersson, 1994). Because males and females of the same species share the majority of their genomes, the genetic basis of sex-specific traits that evolve under sexual selection is poorly understood. It is widely assumed that sexually dimorphic regulation of gene expression facilitates sex-specific adaptations (Connallon and Knowles, 2005; Innocenti and Morrow, 2010; Mank, 2017; Rogers et al., 2020). Recruitment of pre-existing genes or pathways into sexually dimorphic regulatory contexts has been proposed as a remarkable mechanism enabling the divergence of gene expression between the sexes (Kopp et al., 2012; Williams et al., 2008; Tanaka et al., 2011). The sex-differentiation pathway is a conserved switch or regulator governing a set of downstream genes that direct sexually dimorphic traits (Clough et al., 2014; Prakash and Monteiro, 2016). The signaling cascades that transform original gender differences (sex-specific chromosomes) into the alternative splicing of sex differentiation genes (e.g. *Transformer* and *Doublesex* in insects), and the patterns of these genes being spliced into sex-based isoforms have been widely described in different insect orders (Hasselmann et al., 2008; Zhang et al., 2014a; Kiuchi et al., 2014; Herpin and Schartl, 2015; Hall et al., 2015). However, sexually dimorphic traits are usually generated from tightly associated multiple biosynthetic steps that are executed by a series of genes, and the nodes at which sex-determining signals connect with the biosynthetic pathway are poorly understood. Moreover, how these genes are translated into sexually dimorphic traits under elaborate spatial and temporal patterns also needs to be elucidated.

The main function of insect cuticular hydrocarbons (CHCs) is to waterproof the cuticle to resist dehydration under dry conditions (Gibbs, 1998). In many insects, CHCs have been coopted to serve as chemical signals (pheromones) that mediate intraspecific communication (Blomquist and Ginzel, 2021; Howard and Blomquist, 2005). Sexually dimorphic CHC (SDCHC) profiles are widespread in insects (Ingleby et al., 2014; Zhang et al., 2014b; Berson et al., 2019), but the regulatory networks that underlie the formation of SDCHCs largely remain unknown in insects. Considerable works have been done toward the

63 genetic basis of HC biosynthesis and CHC variation in insects. An acetyl-CoA carboxylase catalyzes the
64 biosynthesis of malonyl-CoA, and a cytosolic fatty acid synthase (FAS) incorporates malonyl-CoA units
65 onto the acetyl-CoA primer to form linear long-chain fatty acids (LCFAs). A microsomal FAS catalyzes
66 the biosynthesis of methyl-branched LCFAs using methyl malonyl-CoAs (Juárez et al., 1996; 1992;
67 Blomquist et al., 1995; Parvy et al., 2012; Chung et al. 2014; Wicker-Thomas et al. 2015; Ginzel and
68 Blomquist, 2016). The LCF acyl-CoA can be selectively desaturated by a specific fatty acid desaturase
69 (Desat), leading to unsaturated fatty acids (Chertemps et al., 2006; Legendre et al., 2008). The LCF acyl-
70 CoAs are elongated to form very-long-chain fatty acids (VLCFAs) with specific chain lengths by a fatty
71 acid elongation system, including a rate-limiting elongase (ELO) and three other enzymes (Chertemps et
72 al., 2007; Wicker-Thomas et al., 2015). The VLCF acyl-CoAs are finally reduced to long-chain alcohols by
73 fatty acyl-CoA reductases (FARs) and converted to HCs by the P450 oxidative decarbonylase CYP4Gs
74 (Qiu et al., 2012; MacLean et al., 2018; Li et al., 2019a). It is now clear that the variation in CHCs is
75 primarily reflected in the chain length, number and positions of methyl groups, and the degree of
76 unsaturation, which are determined by ELOs, FASs, and Desats, respectively (Blomquist and Bagnères,
77 2010; Chung and Carroll, 2015; Holze et al., 2020). These genes have been studied in few insect species
78 with regard to SDHCs.

79 In the fruit fly *Drosophila melanogaster*, several studies have elucidated the pheromonal sexual
80 dimorphism of CHCs. Female flies produce C27 and C29 dienes (7,11-heptacosadiene and 7,11-
81 nonacosadiene), and both of them function as female-specific contact sex pheromone components, whereas
82 male flies produce C23 and C25 monoenes (7-tricosene and 7-pentacosene) (Ferveur and Sureau, 1996).
83 Ferveur et al. (1997) found that the targeted expression of a sex-differentiation gene, *Transformer*, in male
84 oenocytes feminized the male CHC profile, and elicited homosexual courtship from other males. These
85 findings implicated sex-differentiation genes in the production of SDHCs. About 10 years later, Chertemps
86 et al. (2006) revealed that the female-specific *desatF* was responsible for the generation of pheromonal
87 dienes in female *D. melanogaster*, and they also found that the sexual dimorphism in HC chain length was
88 modulated by the female-specific *eloF* (Chertemps et al., 2007). The specific expression of *desatF* in *D.*
89 *melanogaster* females was due to a special *cis*-regulatory element (CRE) located upstream of *desatF* in *D.*
90 *melanogaster*; the CRE presented a doublesex protein (Dsx) binding site that could be recognized by the
91 female-specific isoform of *Dsx* (*Dsx-F*), and the binding of Dsx-F activated the transcription of *desatF*,

whereas male-specific Dsx showed no regulatory activity, resulting in sexual dimorphism of *desatF* expression (Shirangi et al., 2009). However, the regulation of other genes involved in the production of SDHCs remains unknown in *D. melanogaster*, and studies in other insects are even rarer.

The German cockroach, *Blattella germanica* is a notorious worldwide indoor pest (Schal, 2011). Considerable works have been done on biochemical aspects of CHCs in *B. germanica* (Chase et al., 1990; Juárez et al., 1992; Schal et al., 1994; Juárez, 2004). CHCs in *B. germanica* function as waterproofing agents (Young et al., 2000), and as importantly, specific HC components are also the biosynthetic precursors for the production of contact sex pheromone components. 3,11-DimeC29 is the most abundant CHC in females. Its hydroxylation at the 2 position, catalyzed by an age- and sex-specific putative cytochrome P450 and further oxidation of the -OH generates the main female-specific contact sex pheromone component, 3,11-DimeC29-2-one (Chase et al., 1992). The contact sex pheromone is an efficient courtship signal. When a sexually mature male's antennae detect the sex pheromone on the female body surface (mainly the antennae), a "fencing" of male and female antennae ensues. The male then rotates his body and orients the abdominal tip toward the female's head, while raising his wings to expose a specialized tergal gland. A mixture of nutrients in the tergal secretion functions as phagostimulants, placing the female in an appropriate position for copulation while she is engaged in feeding on the secretion (Nojima et al., 1999; Eliyahu et al., 2008a; 2009). More recently, Wexler et al. (2019) decoded the alternative splicing patterns of sex-differentiation genes in *B. germanica*. BgTra is only functional in females and can splice *BgDsx* into two non-functional female-specific isoforms ($BgDsx^F$), whereas males generate a complete functional male-type *BgDsx* ($BgDsx^M$). These findings provide opportunities for exploring the mechanisms underlying the SDHCs in *B. germanica*.

In this study, we employed *B. germanica* as a model insect. We characterize the SDCHCs, describe their temporal development, and identify and provide evidence that *BgElo12* is responsible for the formation of SDCHC profiles. In addition, we found that the female-enriched HCs are important in the generation of the female-specific contact sex pheromone; RNAi of *BgElo12* in females decreased courtship responses of males. Moreover, we show that *BgElo12* is under the regulation of the sex-differentiation pathway; $BgDsx^M$ can specifically repress the transcription of *BgElo12*. These findings suggest that the generation of SDHCs is achieved by putting a fatty acid elongation gene (*BgElo12*) under the regulation of

120 *BgDsx*^{M}, and linking the sex-differentiation regulatory cascade with the HC biosynthesis pathway, resulting

121 in the asymmetric gene expression and sexually dimorphic HCs in *B. germanica*.

122

Results

The sexual dimorphism of cuticular hydrocarbons in *B. germanica*

The temporal development of SDCHCs is rarely reported. In order to understand the molecular mechanisms of SDHC generation, we first analyzed the CHC profiles during sexual maturation. The oocytes of female cockroaches mature after eclosion by taking up vitellogenin until ovulation (Schal et al., 1994), and females become sexually receptive and mate 4-5 days before ovulation (Schal and Chiang, 1995). In our study, female cockroaches oviposited late on day 7 or early day 8 (data not shown), therefore AD1–6 (adult days 1-6) adult cockroaches were used for CHC analysis. Different CHC components were identified as previously described (Jurenka et al., 1989). We found no qualitative differences between males and females, but quantitative differences in CHCs became more apparent with adult age (Source data 1). At the early adult stage (AD1 and AD2), females and males showed a similar CHC profile. However, differences were apparent at AD3 and gradually increased until AD6 (Figure 1A). Along with sexual maturation in males, the proportions of C29 CHCs and especially 3,7-; 3,9-; 3,11-DimeC29 (female-enriched peak 24) significantly decreased, while C27 CHCs and 9-; 11-; 13-; 15-MeC29 (male-enriched peak 17) increased. In females, however, the CHC profiles consistently displayed high proportions of C29 CHCs and especially 3,7-; 3,9-; 3,11-DimeC29 (Figure 1B–E). Principal component analysis (PCA) showed that the male and female CHC profiles were more similar at AD1, but diverged at AD6, and the divergence was mainly reflected in the principal component 2 which largely represents the chain length factor (Figure 1F–G). The sexual dimorphism of CHCs was generated at the adult stage (nymphal CHC chromatogram showed no qualitative differences between males and females, Figure 1–figure supplement 1), and the sexes diverged with sexual maturation. Notably, the differences between male and female CHC profiles suggested that chain length is an important factor in sexual dimorphism of CHCs.

BgElo12 and *BgElo24* are involved in HC biosynthesis

The genetic basis of HC production in *B. germanica* is not completely understood. Our previous work identified a fatty acid synthase gene (*BgFas1*) and a P450 oxidative decarbonylase gene (*CYP4G19*) that are involved in HC biosynthesis, but both showed no function in maintaining the sexual dimorphism of CHCs (Pei et al., 2019; Chen et al., 2020). In this study, we found that the differences of CHCs between females

and males are largely reflected in carbon chain length, which suggests that elongase genes may be the crucial regulator of SDCHCs. This was consistent with specific C29 CHCs reported to be enriched in females, and C27 CHCs enriched in males (Wexler et al., 2019). Based on this assumption, we searched for potential *BgElo* genes in the *B. germanica* genomic data and our full length transcriptomic data (Harrison et al., 2018; Pei et al., 2019). A total of 24 different *BgElo* candidate genes were identified, and all *BgElos* were cloned and re-sequenced. Sequence alignment revealed that different BgElo proteins showed high homology and contained the conserved HXXHH and YXYY motifs (Moon et al., 2001). All BgElo proteins displayed a ELO domain and several transmembrane domains (Supplementary file 1).

The fatty acid precursors used for HC production generally originate in the oenocytes, but also can be transported from the fat body to oenocytes (Wicker-Thomas et al., 2015). Therefore, we first analyzed the transcript levels of all *BgElos* in the fat body and abdominal integument. Results showed that *BgElo24* and *BgElo12* were highly expressed in the integument, and *BgElo1*, *2*, *3*, *6*, *7*, *9*, *10*, *11*, *14*, *17*, *20*, and *22* were also abundant in the integument, while other *BgElos* were nearly undetectable (Figure 2A). In the fat body, *BgElo10* and *BgElo22* were highly expressed, *BgElo1*, *2*, *3*, *11*, *12*, and *24* were slightly expressed, and other *BgElos* were undetectable (Figure 2B).

Based on these results, RNAi of the genes that were expressed in the abdominal integument or fat body was performed. A first injection of dsRNA was performed in early fifth-instar nymphs (N5D1 or N5D2), and a boost injection was performed one week later, and then the treated cockroaches were collected at different adult stages and subjected to CHC analysis. RNAi of different *BgElo* genes significantly decreased the mRNA level (Figure 2–figure supplement 1). GC–MS analysis of CHCs showed that C27 CHCs were affected by many genes – knockdown of *BgElo1*, *10*, *12*, *14*, *20*, and *24* caused a significant increase in C27 CHCs, and repression of *BgElo12* showed the greatest increase of the content of C27 CHCs (Figure 2C). C28 CHCs were rarely affected, with only knockdown of *BgElo24* causing a significant decrease in C28 CHCs (Figure 2D). C29 CHCs were the most abundant in *B. germanica*, and only RNAi of *BgElo12* or *BgElo24* significantly decreased their amount (Figure 2E). RNAi of *BgElo12* or *BgElo24* dramatically decreased the amount of C30 CHCs, while RNAi of *BgElo2* increased C30 CHCs (Figure 2F). CHCs with chain lengths greater than 30 occur in low quantities in *B. germanica*, but the most striking result was a sharp decline that resulted from *BgElo24*-RNAi (Figure 2–figure supplement 2). The detailed changes of individual CHCs after RNAi of *BgElos* are available in Source data 2. In conclusion, these data strongly suggest that *BgElo12* and

BgElo24 are involved in CHC production, but we cannot rule out that other *BgElo* genes might have a less prominent role in HC biosynthesis.

***BgElo12* is the terminal gene in maintaining sexually dimorphic hydrocarbon profiles**

Although, it appears that both *BgElo12* and *BgElo24* are involved in HC production, it is unclear which gene is responsible for sexual dimorphism of CHCs. Therefore, we compared the CHC profiles of treated female cockroaches with wild type male cockroaches. The results showed that only RNAi of *BgElo12* made the female CHC profile more similar to the male profile (Figure 3A), reflected by a significant increase of C27 CHCs without affecting the male-enriched peak 17, and a selective downregulation of C29 CHCs, with a dramatic downregulation of the female-enriched peak 24 and some other C29 CHCs (Figure 3B). Also, knockdown of *BgElo12* increased the proportions of C27 CHCs and peak 17, while the proportions of C29 CHCs and peak 24 significantly decreased (Figure 3D). These changes exactly converged the female CHC profile toward the male CHC profile. The repression of *BgElo24* downregulated all C28–C32 CHCs (Figure 3C), even though knockdown of *BgElo24* increased the proportion of C27 CHCs, and decreased the proportion of C29 CHCs and peak 24 (Figure 3E); the amount of the male-enriched peak 17 was also dramatically downregulated (Figure 3C). Similar results were generated in males, and RNAi of *BgElo12* generated the characteristics of male CHC profiles, while *BgElo24*-RNAi downregulated all C28–C32 CHCs (Figure 3–figure supplement1). In order to confirm these results, a second RNAi target was used for both genes, and similar results were generated (Figure 3–figure supplement 2A–B). In addition, we analyzed the internal HCs after repression of *BgElo12* or *BgElo24*. The internal HCs underwent similar changes as CHCs (Figure 3–figure supplement 2C–D). These results suggest that the changes imposed by *BgElo12*- or *BgElo24*-RNAi were caused by a deficiency in *de novo* HC biosynthesis and not the transport of HCs from internal tissues to the cuticle.

We also examined the spatio-temporal expression of *BgElo12* and *BgElo24*. Both *BgElo12* and *BgElo 24* were primarily expressed in the abdominal integument, where the oenocytes that produce HCs are located (Figure 3–figure supplement 3). Monitoring of *BgElo12* expression in females and males across different developmental stages showed that female and male *BgElo12* mRNA levels were similar at N6D4 and early adult stage, but its expression level was higher in females than in males at AD3, and the difference increased through AD6 (Figure 3F), a pattern similar to the production of SDCHCs. The expression levels of *BgElo24*

were higher in males than in females starting at AD2 (Figure 3G). These results also support that only *BgElo12*, and not *BgElo24*, is involved in sexual dimorphism of CHCs in *B. germanica*.

Finally, because CHCs are important waterproofing agents in insects (Gibbs, 1998), we investigated the roles of *BgElo12* and *BgElo24* in desiccation resistance. We found that repression of *BgElo24* dramatically decreased tolerance of desiccation, but RNAi of *BgElo12* had little effect on desiccation tolerance (Figure 3H). These results indicate that the biological significance of *BgElo12* in cockroaches is to support sexual dimorphism of CHCs, whereas *BgElo24* supports desiccation tolerance.

BgElo24 provides VLCFA substrates for BgElo12

Thus far, we showed that both *BgElo12* and *BgElo24* are involved in HC production, RNAi of *BgElo12* only selectively decreased some HCs while repression of *BgElo24* dramatically downregulated all C28–C29 HCs, and some HCs were affected by both *BgElo12* and *BgElo24*. We also found that knockdown of *BgElo24* caused a two-fold upregulation of *BgElo12*, while RNAi of *BgElo12* had no significant influence on *BgElo24* mRNA level (Figure 4–figure supplement 1A–B). Therefore, we considered whether BgElo24 is a basic elongase that provides substrates used for HC biosynthesis, and if BgElo24 generates primary precursors that can be further catalyzed by BgElo12. We verified the functions of BgElo12 and BgElo24 in VLCFA biosynthesis with heterologous expression of *BgElo12* and *BgElo24* in *Saccharomyces cerevisiae* (strain INVSc1). The genetic background of *S. cerevisiae* is relatively clear, as wild type *S. cerevisiae* contains three different ELO proteins: ELO1 is able to elongate C14 FAs to C16 FAs, ELO2 can generate C24 FAs, and ELO3 plays essential roles in the conversion of C24 FAs to C26 FAs (Toke and Martin, 1996; Oh et al., 1997). In our study, activation of GAL1 promoter by galactose successfully transcribed the target genes, and we detected the expression GFP protein (Figure 4–figure supplement 1C–E). GC–MS analysis of FAs in *S. cerevisiae* that contained pYES2-GFP (control) detected large amounts of C16:1, C16:0, C18:1, and C18:0 FAs, minor amounts of C20–C24 and C28 FAs, and a larger amount of C26:0 FAs (Source data 3). Yeast with exogenous *BgElo12* did not produce any new FAs, but heterologous expression of *BgElo24* sharply increased the amount of C28:0 FA, and generated a new component, C30:0 FA (Figure 4A–C; Figure 4–figure supplement 1H–I). These results suggest that BgElo24 is capable of elongating endogenous yeast FAs to generate C28:0 and C30:0 FAs.

Considering that BgElo12 and BgElo24 may selectively elongate substrates with specific carbon chain

lengths, we separately added C20:0, C22:0, C24:0, C26:0, and C28:0 FAs to the medium. Compared with the control, BgElo24 did not produce any new FAs when C20:0, C22:0, C24:0, or C26:0 were added (Source data 3). However, when C28:0 FA was added, yeast with pYES2-BgElo12 generated C30:0 FA, although in small amounts (Figure 4A'–C'; Source data 3). These results suggest that BgElo24 not only directly provides substrates (C28 and C30 fatty acyl-CoAs) for the biosynthesis of C27 and C29 *n*-alkanes, but also provides C28 fatty acyl-CoA for BgElo12 to elongate to C30 fatty acyl-CoA, which in turn generates C29 *n*-alkane. This might be the reason why *in vivo* RNAi of *BgElo12* slightly decreased C29 *n*-alkane and caused a dramatic increase in C27 *n*-alkane, whereas RNAi of *BgElo24* dramatically decreased C29 *n*-alkane. In order to analyze the activity of BgElo12 and BgElo24 in elongating methyl-branched FAs, two representative substrates, 2-MeC16:0 and 14-MeC16:0 FAs, the potential substrates for 15-methyl HCs and 3-methyl HCs, respectively, were added to the medium. However, we found that these substrates could not be catalyzed by BgElo12 or BgElo24 (Figure 4–figure supplement 1F–F'' and 1G–G''). We suspect that this might be caused by a shortcoming of the yeast FA elongation system. FA elongation requires an elongase and three other enzymes including a 3-keto-acyl-CoA-reductase, a 3-hydroxy-acyl-CoA dehydratase, and a trans-enoyl-CoA-reductase (Wicker-Thomas et al., 2015). The last three yeast endogenous enzymes may not catalyze methyl branched substrates. In conclusion, these results indicate that both BgElo12 and BgElo24 catalyzed the biosynthesis of VLCFAs in the yeast heterologous system, and BgElo24 was able to provide primary substrates for BgElo12. However, the activity of BgElo12 and BgElo24 in methyl-branched FA elongation needs further investigation.

Female-enriched HCs are crucial for contact sex pheromone-based courtship performance

The largest single chromatographic HC peak in females contains 3,7-; 3,9-; 3,11-DimeC29, which is much less represented in males. Because 3,7-; 3,9-; 3,11-DimeC29 has been shown to be the precursor for the contact sex pheromone 3,11-DimeC29-2-one (C29 methyl ketone) in *B. germanica* (Chase et al., 1992), we suspected that the female-specific HC profile may be important for maintaining a high level of contact sex pheromone. We first monitored the pattern of 3,11-DimeC29-2-one accumulation in the first gonotrophic cycle. The contact sex pheromone showed a stable low level at the early adult stage (AD0–AD2), its accumulation started at AD3, quickly increased from AD5 to AD7 (Figure 5A), but decreased at AD8 when

most females oviposited (data not shown). Analysis of the influence of *BgElo12*-RNAi on C29 methyl ketone was performed at AD6. Female cockroaches were subjected for three consecutive dsRNA injections before being subjected to lipid analysis: the first one at early fifth instar, the second one at early sixth instar, and the third one at AD1. We found that repression of *BgElo12* reduced the C29 methyl ketone by more than 75% in both cuticular and internal extractions (Figure 5B–D).

We next determined whether the *BgElo12*-RNAi repression of pheromone production in females affected male courtship behavior. When the female contact sex pheromone is detected by a male, it displays a characteristic male courtship behavior, including wing-raising (WR) (Eliyahu et al., 2008a). Importantly, this behavior can be elicited by an isolated female antenna, and details of this assay, including latency and rate of WR, have been described (Wada-Katsumata and Schal, 2019). When an antenna of AD5 female was used as stimulus, nearly all males responded. RNAi of *BgElo12* resulted in only a slight decline in WR rate (about 20%), but the latency of WR was significantly increased (Figure 5E and 5E'). AD5 females accumulated a large amount of contact sex pheromone, whereas males can be fully activated by about 10 ng of 3,11-DimeC29-2-one applied onto an antenna (Schal et al., 1990). This is likely the reason why RNAi of *BgElo12* had only a small influence on WR rate. Therefore, we repeated this experiment using AD3 females, which have less contact sex pheromone on the cuticle. We found that males responded to 80% of the control antennae with the WR display, but less than 40% of the antennae from *BgElo12*-RNAi females elicited WR in males. The average latency of WR toward antennae of *BgElo12*-RNAi females was 18.03 s, while the control antennae elicited WR in 11.05 s (Figure 5F and 5F'). These results indicate that the female-enriched HCs are advantageous for contact sex pheromone biosynthesis, especially at the early sexual maturation stage.

Sex-differentiation genes modulate *BgElo12*

The female-enriched HC composition is tightly associated with a higher expression of *BgElo12* in females, but the regulators that govern sexually dimorphic expression of *BgElo12* in females and males are unknown. Wexler et al. (2019) reported that RNAi of the sex-determination gene *BgTra* in females converts its CHC profile to a male-like profile. Taken together with our results, it would appear that the sex-differentiation pathway might be involved in regulating *BgElo12* expression. We first confirmed the function of *BgTra* and *BgDsx* in sex-specific development *via* RNAi. For each gene, we used two unique RNAi targets within a conserved sequence region for multiple isoforms. RNAi of *BgTra* and *BgDsx* in females or males

showed similar phenotypes as described by Wexler et al. (2019). *BgTra* is only functional in females, while *BgDsx* only works in males (Figure 6–figure supplement 1). We next studied the expression of *BgTra* and *BgDsx* in females and males using qPCR primers that target all isoforms of each gene. The expression of both *BgTra* and *BgDsx* increased after eclosion, but *BgTra* transcript levels tended to be stable from AD4 to AD6 (Figure 6A–B). RNAi of *BgTra* in females significantly decreased the mRNA level of *BgElo12*, but *BgElo12* expression was unaffected in males (Figure 6C). Notably, the downregulation of *BgElo12* by ds*BgTra*-injection in females could be rescued by co-injection of ds*BgTra* and ds*BgDsx* (Figure 6C), but ds*BgDsx* alone was not functional in regulating *BgElo12* expression in females (Figure 6D). Conversely, in males, knockdown of *BgDsx* alone increased the expression of *BgElo12* (Figure 6D). According to Wexler et al. (2019), RNAi of *BgTra* in females generated the male type *BgDsx* ($BgDsx^{M}$). We suspect that the downregulation of *BgElo12* in females after RNAi of *BgTra* was caused by the generation of $BgDsx^{M}$. This hypothesis was supported by co-injection of ds*BgTra* and ds*BgDsx*, and a dual-luciferase reporter assay that $BgDsx^{M}$ could directly modulate the expression of *BgElo12* by interaction with its upstream sequence region (Figure 6-figure supplement 2). Further, we found that RNAi of neither *BgTra* in females nor *BgDsx* in males could affect the expression of *BgElo24* (Figure 6–figure supplement 3), suggesting that *BgElo24* is not regulated by these two sex-differentiation genes.

We further analyzed the effects of *BgTra* and *BgDsx* on HC profiles. Knockdown of *BgTra* in females masculinized the CHC profile and increased the male-enriched CHC components; however, this change disappeared by co-injection of ds*BgTra* and ds*BgDsx* (Figure 6E–F, and Figure 6–figure supplement 4A). Similarly, repression of *BgDsx* in males feminized the CHC profile, and increased the female-enriched components (Figure 6E, 6G, and Figure 6–figure supplement 4B). In order to verify that the sex-differentiation genes affected CHC profiles by regulating the generation of HCs but not their selective transport and deposition to the cuticle, we analyzed the internal HCs. RNAi of both *BgTra* in females and *BgDsx* in males caused an inter-sexual conversion of internal HC profiles, as seen in the CHCs (Figure 6–figure supplement 5A–D). Although we found little qualitative differences in the HC profiles between internal and cuticular HCs, we found significant quantitative changes. For example, after RNAi inhibition of *BgTra* in females, the increase of 9-; 11-; 13-; 15-MeC29 (peak 17) on the epicuticle was greater than internal tissues, while the decrease of 3,7-; 3,9-; 3,11-DimeC29 (peak 24) in surface was less than internal tissues (Figure 6–figure supplement 4A and Figure 6–figure supplement 5A). Suggesting the possibility of excessive

transport of internal HCs toward the cuticle after repression of *BgTra* in females. As for RNAi of *BgDsx* in males, an opposite change was generated – there appeared to be less transport of HCs to the cuticle (Figure 6–figure supplement 4B, Figure 6–figure supplement 5B). Also, the total amount of internal HCs was significantly decreased in *BgTra*-RNAi females, while it was increased in *BgDsx*-RNAi males (Figure 6–figure supplement 5E and 5F). These results suggest there is an unusual transport of HCs after repression of *BgTar* or *BgDsx*. We suspect that the unusual transport of HCs may be caused by changes in the capacity to store internal HCs, as large amounts of internal HCs are shunted to the ovaries (Schal et al., 1994; Gu et al., 1995), and sex-differentiation genes are the key regulators of normal ovary development in females and repression of ovary generation in males (Kopp, 2012; Wexler et al., 2019). We conclude that although the transport of HCs from internal tissues to the cuticle was affected after repressing *BgDsx* or *BgTra*, the effect was on overall HC transport, with no apparent selective transport on specific HCs.

Overall, our results indicate that the sexual dimorphism of HCs in *B. germanica* is primarily determined by *BgElo12*, and sex-determination pathway genes are the critical regulators that control the asymmetric expression of *BgElo12* between males and females.

Discussion

Our study reveals a novel molecular mechanism responsible for the formation of SDHCs in *B. germanica*. The CHC profiles in insects are regulated by complex biosynthetic and transport pathways, involving multiple gene families. We demonstrated that a fatty acid elongation step is responsible for sexual dimorphism of CHCs in *B. germanica*, the female-enriched *BgElo12* is the core gene that encodes for the elongase involved in generating more female-enriched HCs, and the asymmetric expression of *BgElo12* between the sexes is modulated by sex-differentiation genes: $BgDsx^{M}$ represses the expression of *BgElo12* in males, while *BgTra* removes this repression in females. Because a female-enriched HC serves as a precursor to a female contact sex pheromone, we also revealed the prominence of *BgElo12* in sexual behavior.

Fatty acid chain elongation is a key step in the regulation of sexually dimorphic HCs in *B. germanica*

The diversity of HCs in insects is reflected in the HC carbon chain lengths, their degree of saturation, and the number and positions of methyl groups (Holze et al., 2020). HCs in *B. germanica* are composed of only alkanes and methyl-branched alkanes, and the fatty acid biosynthesis gene that governs the incorporation of methyl groups in the aliphatic chain showed no role in generating the sexual dimorphism of HCs in *B. germanica* (Pei et al., 2019). In this study, we found that sexually mature female cockroaches contain relatively higher amounts of C29 HCs than males, whereas male cockroaches had more C27 HCs, suggesting that chain length is an important factor in the dimorphism of HCs.

Studies of the genetic bases of HC biosynthesis in insects have demonstrated that chain lengths are determined by the fatty acid elongation process: the rate-limiting enzyme elongase determines the chain lengths of VLCFA products, and produces the final HCs with different chain lengths (Ginzel and Blomquist, 2016). In our study, an RNAi screen identified that *BgElo12* and *BgElo24* were involved in HC biosynthesis. Expression of both genes in yeast demonstrated that both BgElo12 and BgElo24 displayed functions similar to ELOVL4 in mammals, which showed a special function in the biosynthesis of VLCFAs with chain lengths greater than C28 (Ohno et al., 2010). *BgElo24*, however, is a more fundamental elongase that seems able to catalyze a wide range of substrates to generate FAs of various chain lengths, and can also provide primary substrates for BgElo12 to produce C30 FAs. Notably, only *BgElo12* had higher expression in females, which

was consistent with the higher amounts of C29 HCs in females. Knockdown of *BgElo12* in females caused a dramatic decrease of the female-enriched peak 24 (3,11-DimeC29) but it did not affect the male-enriched peak 17 (9-; 11-; 13-; 15-MeC29), which generated a male-like HC profile; however, RNAi of *BgElo24* unselectively downregulated all C28–30 HCs, indicating that only *BgElo12* was involved in the formation of SDHCs in *B. germanica*. Lastly, we found both RNAi of *BgElo12* and *BgElo24* increased some C27 HCs, indicating that there are some other *BgElos* involved in HC production. The identification of these genes will be arduous, because the C27 compounds occur in small amounts, and multiple BgElos may catalyze the synthesis of the same HC independently. It is worth noting in this regard that *Blattella asahinai*, a sister species of *B. germanica* produces almost no C27 compounds (Pfannenstiel et al. 2008). These two species can hybridize, potentially offering a resource for the genetic regulation of C27 HCs.

In *B. germanica*, as in other insects, HCs are transported through the haemolymph and selectively incorporated into or deposited on various tissues, including the cuticle, ovaries and specialized pheromone glands (Young et al., 2000; Schal et al., 2001; Schal et al. 1998). In our study, analysis of the influence of *BgElo12*-RNAi on internal HCs demonstrated that the female- and male-specific CHC profiles were not caused by selective transport, but rather by differences in *de novo* HC biosynthesis between the sexes, regulated by *BgElo12*. Elongases have been shown to participate in HC production in several other insect species including *D. melanogaster*, *Nilaparvata lugens*, and *Locusta migratoria* (Chertemps et al., 2007; Li et al, 2019b; Zhao et al., 2020). The elongase gene *eloF* was also shown to be specifically expressed in females, and might be associated with the sex-differentiation gene *Transformer*, but the reason why it cannot be transcribed in male flies is not very clear (Chertemps et al., 2007). Nevertheless, the roles of elongase genes in sexual dimorphism of HCs in other insects have not been described.

BgElo12 **and** ***BgDsx^{M}*** **are key nodes connecting the hydrocarbon synthesis and sex-differentiation pathways**

In this study, we first demonstrated that *BgElo12* is the key regulator in the HC biosynthesis pathway, responsible for the differences in the HC profiles between females and males. We next explored the upstream regulators that modulate the sexually dimorphic expression of *BgElo12*. The molecular genetic switches that determine which sex-determination pathway is followed by males and females are highly variable in animals. The *doublesex/mab-3 related* (*Dmrt*) family of transcription factors includes conserved developmental

regulators in the sex-differentiation pathway, governing the fate of sexually dimorphic traits in animals (Kopp, 2012). *Doublesx* (*Dsx*) in arthropods, which is related to *Dmrt*, works through sex-specific splice variants that are controlled by *Tra* in many insects. Sex-specific *Dsx* isoforms promote sexual differentiation by modulating diverse downstream genes; thus, the *Dsx* gene is regarded as a central nexus in sexual differentiation (Gempe and Beye, 2011; Verhulst and van de Zande, 2015). Previous work reported that knockdown of *BgTra* converted the female cockroach CHC profiles to male-like profiles (Wexler et al., 2019). In our study, RNAi of *BgTra* in female cockroaches indeed downregulated the expression of *BgElo12*, but the effect of *BgTra*-RNAi on *BgElo12* expression could be recovered by co-injection of ds*BgTra* and ds*BgDsx*, and RNAi of *BgDsx* in males upregulated *BgElo12* transcripts. These results suggest that $BgDsx^{M}$ can repress the transcription of *BgElo12* in males, and the downregulation of *BgElo12* by repressing *BgTra* was caused by the conversion of $BgDsx^{F}$ to $BgDsx^{M}$, as *BgTra* is able to regulate the splicing of $BgDsx^{M}$ to $BgDsx^{F}$ (Wexler et al., 2019). The regulation of *BgDsx* on *BgElo12* thus connects the sex-differentiation pathway with the HC biosynthesis pathway, and therefore enables the sexual dimorphism of HCs in *B. germanica*.

Although the dual-luciferase reporter gene assay suggested that $BgDsx^{M}$ can directly regulate the transcript of *BgElo12*, there may be other indirect regulatory pathways. Several candidate factors have been shown to regulate the HC profiles in various insects (e.g., *D. melanogaster*), including ecdysone, juvenile hormone (JH), biogenic amine, and the insulin signaling pathway (Wicker et al., 1995a; 1995b; Marican et al., 2004; Kuo et al., 2012; Bontonou et al., 2015; Fedina et al., 2017; Baron et al., 2018). These connections are highlighted by ecdysone, which is mainly produced by the prothoracic gland, but in some insects also by the ovaries (Bownes and Smith, 1984; Romaá et al., 1995), and the development of the ovaries is under the regulation of the sex-differentiation pathway. Moreover, endocrine signals like JH and insulin are also regulated by the sex-differentiation pathway (Zinna et al., 2018). Therefore, these signals may be potential mediators that complete the regulatory network between *BgDsx* and *BgElo12*. However, more detailed investigations are needed to thoroughly elucidate the differential regulation of HC production in both females and males.

Dsx also regulates the HC biosynthesis pathway in *D. melanogaster*; Dsx^{F} specifically activates the transcription of *desatF* and generates pheromonal dialkenes (Shirangi et al., 2009). In *B. germanica*, *BgDsx* operates differently in that $BgDsx^{M}$ suppresses female traits in male cockroaches, and *BgTra* is important in

removing this inhibitory effect in females (Wexler et al., 2019). Thus, *BgDsx*^{M} represses the expression of *BgElo12*, and therefore it represses the generation of female-enriched HCs in males, and *BgTra* is crucial in maintaining female-enriched HCs, especially for the contact sex pheromone precursors. However, *BgTra* affects contact sex pheromone biosynthesis in female cockroaches through additional pathways. We found that RNAi of *BgTra* in females dramatically decreased the expression of the JH-responsive *Krüppel homolog 1*, *Krh1*, a zinc-finger transcription factor (Figure 6–figure supplement 6). JH can activate the expression of a putative sex-specific and rate-limiting cytochrome p450 that catalyzes the hydroxylation of 3,11-DimeC29 to 3,11-DimeC29-alcohol, which is then oxidized to the methyl ketone pheromone (Chase et al., 1992; Lozano and Belles, 2011), and we found that JH performed this function *via Krh1* (our unpublished data). Therefore, the influence of *BgTra* on contact sex pheromone biosynthesis is explained not only by its effects on precursor synthesis, but also for the transition of precursors to methyl ketones.

Biological significance of the sexual dimorphism of HCs

Sexually dimorphic traits are generated in females and males in response to intra- and inter-sexual selection, but pleiotropic traits are also subject to natural selection, especially when they are also shaped by and adapted to environmental stresses (Andersson, 1994; Kunte, 2008). Most insect sex pheromones are C12-18 aldehydes, alcohols and acetate esters, derived from fatty acids in specialized pheromone glands. These pheromones appear to have no other function beyond attracting the opposite sex. In contrast, CHC pheromones appear to serve both in sexual communication and in waterproofing of the cuticle. The female-specific contact sex pheromone of *B. germanica* is clearly subject to both natural and sexual selection because it is derived from a prominent CHC, which also serves as a waterproofing component of the CHC profile and is maternally invested in offspring (Fan et al., 2008). Thus, maintenance of HC contact sex pheromone precursors in female cockroaches is adaptive in both reproductive success and survival in an arid environment. The quality of insect pheromones is considered an honest indicator of fitness potential (Kuo et al., 2012). This assertion may be particularly pertinent in *B. germanica*, where the pheromone and its HC precursor serve in sexual communication, resilience to environmental stressors, and in maternal investment in eggs.

In systems that use CHCs in sexual communication, it is common for the CHC profiles to contain female- and male-specific components, as is evident in *Drosophila*. In *B. germanica*, as well, male cockroaches have a unique CHC profile, especially enriched in C27 components with 9-; 11-; 13-; 15-MeC29

being particularly prominent. The male-specific HC profile is generated during sexual maturation, suggesting that it may function in sexual communication. It is possible that the male-enriched 9-; 11-; 13-; 15-MeC29 may function as a sex pheromone in three related contexts: a) it may distinguish males and females within cockroach aggregations; b) it may signal "maleness" and male quality to females; and c) it may function in male-male recognition, contests and competition for access to females. Moreover, it is possible that male-specific P450s may catalyze the oxidation of these male-enriched HCs to homologous methyl ketones, as in females, and in turn serve these functions. However, more bioassays are required to analyze the biological significance of male-specific CHC profiles.

Materials and Methods

Insect rearing

The German cockroach, *Blattella germanica* originated from a laboratory strain collected in the 1970s. The cockroaches were maintained in aquaria at 30 ± 1ºC with a relative humidity (RH) of ~ 50% under 12: 12 h light–dark photoperiod regime, and fed rat chow and tap water. Newly hatched cockroaches were separated and reared in new containers. Early stage (day 1 or 2) fourth- and fifth-instar nymphs were separated and used in dsRNA injection; newly emerged adults were collected and reared in plastic jars for experiments.

Preparation of HCs and methyl ketones

Blattella germanica cuticular lipids were extracted following Gu et al. (1995) with slight modifications. Individual adult female cockroaches were sacrificed by freezing at −20ºC, and then thawed at room temperature. Cuticle surface-extracted in 1 mL of hexane twice, and finally rinsed in 1 mL of hexane. *n*-Hexacosane (15 μg) or 14-heptacosanone (0.5 μg) were added as internal standards. The extracts were combined and reduced to ~300 μL with a nitrogen flow and loaded onto a Pasteur pipette mini-column, as previously described (Pei et al., 2019). The cuticular hydrocarbons were eluted with 8 mL of hexane, and the contact sex pheromone fraction was subsequently eluted with 8 mL of 3% ethyl ether in hexane. Internal lipids were extracted from the cockroach following a procedure described by Fan et al. (2002) with slight modifications. Each surface-extracted cockroach was homogenized in a solution of hexane–methanol–ddH2O (2:1:1 mL), 30 μg of *n*-hexacosane and 1 μg of 14-heptacosanone were added for quantification of internal HCs and methyl ketones, respectively. The homogenate was vigorously vortexed and centrifuged at 2500 g for 10 min. The supernatant hexane phase was collected and the extraction was repeated using n-hexane. Separation of HCs and methyl ketones was performed using column chromatography, as described above.

Gas chromatography–mass spectrometry (GC–MS) analysis

Lipid analysis was performed with a TRACE 1310 GC–ISQ single quadrupole MS (Thermo Fisher Scientific, Waltham, MA, USA). In brief, lipids were separated on a DB-5MS capillary column (30 m length,

0.25 mm ID, 0.25 μm film thickness; Agilent Technologies, Santa Clara, CA, USA). The oven started at 60°C and kept for 2 min, heated to 160°C for HCs and methyl ketones, or 220°C for fatty acid methyl esters (FAMEs) at a rate of 30°C/min, then increased at 3°C/min up to 250°C, followed by 10°C/min up to 320°C and held for 5 min. Electron ionization mode (70 eV) was used, and the MS scan range was 45–650 m/z at a rate of 5 scans/s. Identification of compounds and peak area determination was performed with a Xcalibur 2.2 workstation.

RNA isolation and real time-quantitative PCR (RT-qPCR)

Total RNA was isolated with RNAiso Plus Reagents (Takara, Dalian, Liaoning, China) according to the manufacturer's instructions. cDNA was reverse-transcribed from 800 ng of total RNA using the PrimeScript™ RT reagent Kit with gDNA Eraser (Takara). Gene-specific primers with appropriate amplification efficiency (0.95–1.05) were screened by a cDNA dilution series (Supplementary file 2). Quantification of gene expression level was performed with TB Green™ Premix Ex Taq™ Tli RNase H Plus (Takara) on a LightCycler 480 system (Roche). Target genes expression was normalized by the commonly used housekeeping gene *actin5c* (GenBank: AJ862721.1) and calculated using the $2^{-\Delta\Delta Ct}$ method (Livak and Schmittgen, 2001). Each treatment contained four biological replicates and technical triplicates.

Identification of *BgElo* gene family members

Both BLASTN and BLASTP were used to search *BgElo* genes in *B. germanica* genome data (Harrison et al., 2018) and our own full-length transcriptome data (NCBI accessions: SRR9143014 and SRR9143013) using the homologous genes of *Elongase* from *D. melanogaster* as query sequences. Candidate *BgElo* genes were amplified with the PrimeSTAR GXL DNA Polymerase reagent (Takara) (primers are listed in supplementary file 2), the amplified fragments were inserted into the pMD™ 19-T Vector (Takara) and re-sequenced. Candidate *BgElo* genes were then translated and submitted to SMART online tools (http://smart.embl-heidelberg.de) to analyze the conserved structures; only genes with the typical ELO domain were confirmed as *BgElo* genes. The putative *BgElo* mRNA sequences were mapped to the genomic data (GenBank: PYGN00000000.1) using a local BLASTN tool (Altschul et al. 1990), and the intron-exon structure was analyzed based on the GT-AG rule. The conservative motifs in *BgElos* were analyzed by sequence alignment with DNAMAN 9.0 software.

Expression profile analysis

In order to screen the potential *BgElo* genes involved in HC biosynthesis, the expression levels of different *BgElo* genes were quantified in the fat body and abdominal integument, where HCs or their precursors were generated. In addition, other tissues including the head, thorax, gut, legs, ovaries, Malpighian tubules, ejaculatory duct (from two-day-old males), and colleterial glands were dissected from two-day-old females, and were used to analyze the expression profiles of *BgElo12* and *BgElo24* among different tissues. In order to study the time course of *BgElo12*, *BgElo24*, *BgDTra*, and *BgDsx* transcript levels during sexual maturation, a representative nymphal stage (four-day-old sixth-instar nymph, N6D4) and AD0–AD6 females and males were collected. Total RNA was extracted from various tissues or intact cockroaches, and the expression profiles of different genes were studied *via* RT-qPCR.

Transcript knockdown *via* RNAi

Gene-specific target sequences as well as a heterologous fragment from *Mus musculus* (Muslta) used for double-stranded RNA (dsRNA) synthesis were amplified and cloned into pMD^{TM} 19-T Vector (Takara). Templates used for single-stranded RNA was amplified with primers that were embedded with the T7 promoter sequence (Supplementary file 2). Different kinds of dsRNA were subsequently generated with the T7 RiboMAX™ Express RNAi System (Promega). Delivery of dsRNA was performed with a Nanoject II micro-injector (Drummond Scientific) for fourth-instar cockroaches and microliter syringes for fifth-, sixth-instar, and adult cockroaches. For RNAi screen of *BgElo* genes in HC biogenesis, a double injection strategy was employed: the first injection was performed at the early fifth-instar (one- or two-day-old fifth-instar, N5D1-N5D2) with a dosage of 3 μg in 2 μL; the second injection was performed one week later with a dosage of 4 μg in 2 μL. For confirming the function of *BgElo12* in contact sex pheromone biosynthesis, a third injection with 4 μg of dsRNA in 2 μL was carried out on one-day-old adults (AD1), and methyl ketones were extracted at AD6. Knockdown of sex-determination genes was accomplished with three dsRNA injections, the first at early fourth instar (N4D1-N4D2), the second at early fifth instar (N5D1-N5D2), and the last at early sixth instar (N6D1-N6D2). The fourth-instar cockroaches were injected with ~0.5 μg of dsRNA in ~0.2 μL; the fifth- and sixth-instar cockroaches were injected with 1 μg of dsRNA in 2 μL. In order to verify the function of *BgElo12* and *BgElo24* in HC biosynthesis and sex-determination genes in

549 modulating *BgElo12* mRNA levels or HC profiles, two non-overlapping gene-specific targets were designed
550 and used in this study, as there are some isoforms of *BgDsx* and *BgTra*, the RNAi targets were designed
551 within the common sequence region according to Wexler et al. (2019).
552
553 **Heterologous expression and fatty acid analysis**
554 Heterologous expression was performed according to Hastings et al. (2001) with slight modifications.
555 Complete coding sequences (CDS) of *BgElo12*, *BgElo24*, or control (*GFP*) were amplified with
556 PrimeSTAR® HS DNA Polymerase (Takara) using the gene-specific primers (Supplementary file 2) that
557 contain the restriction enzyme sites (*KpnI* and *BamHI* for *BgElo12* and *BgElo24*; *BmHI* and *EcoRI* for *GFP*)
558 and the yeast consensus sequence (TACACA) following the restriction enzyme sites (only for forward
559 primers). The amplified *BgElo12*, *BgElo24*, or *GFP* CDS fragments were ligated into the linearized pYES2
560 shuttle plasmid (Thermo Fisher Scientific) and verified by sequencing. The recombinant plasmids were
561 transformed into INVSc1 *Saccharomyces cerevisiae* (Thermo Fisher Scientific) using the PEG-LiAc method,
562 and streaked onto *S. cerevisiae* minimal medium minus uracil (SC-Uracil) plates to select transformants;
563 single colonies were inoculated in SC-Uracil medium with 2% glucose. After culturing at 30℃ for 24 h, the
564 yeast was collected and diluted to an OD600 of 0.4 with SC–Uracil medium containing 1% raffinose and 2%
565 galactose, and further cultured at 30℃ until they reached an OD600 of 0.8. At this point, transcription of
566 exogenous genes was examined by RT-PCR. Substrates of C20 (0.5 mM), C22 (1 mM), C24 (1 mM), C26
567 (1 mM), C28 (1 mM), 2-methylhexadecanoic acid (0.5 mM), and 14-methylhexadecanoic acid (0.5 mM)
568 were separately added into the cultures with an extra 1% of tergitol type Nonidet P-40. All the substrates
569 were purchased form Sigma-Aldrich (Louis, MO, USA) or TCI (Shanghai, China).
570 After 48 h, yeast cells were harvested by centrifugating at 500 g for 5 min and washed thrice with Hank's
571 balanced salt solution for fatty acid derivatization and analysis. Pellets were dried under a steam of nitrogen
572 and 2 mL of 1% (v/v) H_2SO_4 in methanol was added, the mixture was vortexed and incubated at 80 °C water
573 bath in a N_2 atmosphere for 2 h (Lepage and Roy, 1984). After that, 1 ml of saturated sodium chloride solution
574 was added into the mixture and FAMEs were extracted with 1 mL of hexane for three times. The FAME
575 extracts were concentrated and subjected to GC–MS analysis as described above. Different FAMEs were
576 identified by comparison to FAME standards (purchased from Sigma-Aldrich) and their mass spectra.
577

Desiccation bioassay

The capacity of *BgElo12* and *BgElo24* in water retention was assessed by a desiccation bioassay. Drying bottles were prepared by putting ~120 g of packed fresh silica gel into a ~900 mL sealed plastic bottle. The RH inside the bottle dropped to 5% within 2 h which was monitored by HOBO Pro v2 (Onset, Bourne, USA). AD2 females were injected with ds*BgElo12*, ds*BgELo24*, and ds*Muslta* and separately caged in the desiccation bottles at 30℃, supplied with ~1 g of dry food, but no water. Survival was recorded every 8 h until all the cockroaches died. About 100 cockroaches were used for each treatment.

Courtship behavioral study

Courtship behavior was tested according to Eliyahu et al. (2008b) with slight modifications. Antennae from differently treated AD3 or AD5 females were excised, and each antenna was attached on the tip of a glass Pasteur pipette with paraffin, the antenna was used immediately to test the responses of AD13–15 males that were separated from females since eclosion. The test antenna was used to touch the antennae of the male, and a positive response was recorded if the male cockroach turned its body and raised wings to approximately 90 degrees within 30 sec. A negative response was recoded if the test antenna failed to elicit a response in a male cockroach and this male then responded to a positive control antenna from a normal AD6 female. The wing raising (WR) latency was recorded according to Wada-Katsumata and Schal (2019); the latency of the WR display was timed from contact of the antennae to the initiation of the male WR display. All female antennae and male cockroaches were used only once, all tests were performed in the scotophase and we avoided the first and last 2 h of the scotophase. Bioassays were conducted under a dim red light to simulate a dark environment.

Dual-luciferase reporter gene assay

The 5’ end of *BgElo12* was obtained by 5’ Rapid Amplification of cDNA Ends (RACE), 5’ RACE cDNA library was prepared using Clontech SMARTer RACE 5'/3' Kit (Takara) according to the user manual with the gene-specific primer (Supplementary file 2) and kit-provided Universal long primer. The amplified fragments were cloned into pRACE vector and sequenced. About a 2.7 kb sequence upstream of *BgElo12* was amplified and cloned into pGL3-basic vector, and the CDS sequences of $BgDsx^{M}$ and GFP (control)

were separately cloned into the expression vector pCDNA3.1. The HEK293T cells were cultured in a 24-well plate with 500 μL of DMEM medium (Thermo Fisher Scientific) for 24 h before transfection, and the restructured pGL3-basic vector (200 ng/well) was co-transfected with the expression vectors (200 ng/well) to HEK293T cells using Lipofectamine^{TM} 3000 (Invitrogen, Carlsbad, CA, USA). The pRL-TK that encoded a Renilla luciferase was also co-transfected as an internal control. The transfected cells were cultured at 37°C for 36 h and subjected to luciferase activity analysis using the Dual-Glo Luciferase Assay System (Promega, Madison, WI, USA).

Statistics

Data were statistically analyzed using SPSS 23 and presented as mean ± SEM or mean ± SD. Two-tailed Student's *t*-test was used for two-group comparison; and significant differences between multi-groups are analyzed by one-way ANOVA followed by the LSD test (Equal variances assumed) or Welch's ANOVA followed by Games-Howell multiple comparisons test (Equal variances not assumed) at $P < 0.05$ level. Principal component analysis (PCA) was used to distinguish the CHC profiles of AD1 and AD6 cockroaches.

Acknowledgments

We thank Shan-Wang Hong from Northwest A&F University for his help in sequence analysis. This work was supported in part by the National Natural Science Foundation of China to YLF (Grant No. 31772533), the United States National Science Foundation (IOS-1557864), the Blanton J. Whitmire Endowment at North Carolina State University to CS, and the Special Fund of Northwest A&F University to TXL (NWAFU-2009-01-001-TXL).

Competing interests: The authors declare that no competing interests exist.

Additional information

Funding

Funder	Grant reference number	Author
National Natural Science Foundation of China	Grant No. 31772533	Yong-Liang Fan
United States National Natural Science	IOS-1557864	Coby Schal
Northwest A&F University Special Fund	2009-01-001-TXL	Tong-Xian Liu

The funders had no role in study design, data collection and interpretation, or the decision to submit the work for publication.

Author contributions

XJP, Conceptualization, Methodology, Investigation, Collection and analysis of data, Writing—original draft, Writing—review and editing; YLF, Funding acquisition, Conceptualization, Project administration, Writing—review and editing; YB, TB, ZFZ, NC, Methodology, Investigation, Writing—review and editing; SC, Funding acquisition, Conceptualization, Writing—review and editing; SL, Resources, Methodology, Writing—review and editing; TXL, Funding acquisition, Resources, Supervision, Project administration,

642 Writing—review and editing.

643

644 ## Author ORCIDs and Emails:

645 **Tong-Xian Liu: txliu@nwafu.edu.cn, 0000-0002-7686-0686**

646 **Yong-Liang Fan: yfan@nwafu.edu.cn, 0000-0002-7993-2497**

647 **Xiao-Jin Pei: xiaojinpei@nwafu.edu.cn, 0000-0003-4311-6954**

648 **Coby Schal: coby@ncsu.edu, 0000-0001-7195-6358**

649

650 ## Data availability

651 PacBio data sets have been deposited in NCBI's SRA under the accession numbers SRR9143014 and

652 SRR9143013. All *BgElo* sequences have been submitted to NCBI's GenBank under the accession numbers

653 MT925720 and MW380216–MW380238

654

655 ## Additional files

656 **Supplementary file 1.** Sequence alignment and protein structure analysis of BgElos.

657 **Supplementary file 2**. Primer sequences used in this study.

658

References

Altschul SF, Gish W, Miller W, Myers EW, Lipman DJ. 1990. Basic local alignment search tool. *J Mol Biol* 215:403–410. DOI: https://doi.org/10.1016/S0022-2836(05)80360-2.

Andersson M. 1994. Sexual selection. Princeton, NJ: Princeton University Press.

Baron A, Denis B, Wicker-Thomas C. 2018. Control of pheromone production by ovaries in *Drosophila*. *J Insect Physiol* 109:138–143. DOI: https://doi.org/10.1016/j.jinsphys.2018.07.003.

Bear A, Monteiro A. 2013. Both cell-autonomous mechanisms and hormones contribute to sexual development in vertebrates and insects. *BioEssays* 35:725–732. DOI: https://doi.org/10.1002/bies.201300009.

Berson JD, Simmons LW. 2018. A costly chemical trait: phenotypic condition dependence of cuticular hydrocarbons in a dung beetle. *J Evol Biol* 31:1772–1781. DOI: https://doi.org/10.1111/jeb.13371.

Berson JD, Garcia-Gonzalez F, Simmons LW. 2019. Experimental evidence for the role of sexual selection in the evolution of cuticular hydrocarbons in the dung beetle, *Onthophagus taurus*. *J Evol Biol* 32:1186–1193. DOI: https://doi.org/10.1111/jeb.13519.

Blomquist GJ, Tillman JA, Reed JR, Gu P, Vanderwel D, Choi S, Reitz RC. 1995. Regulation of enzymatic activity involved in sex pheromone production in the housefly, *Musca domestica*. *Insect Biochem Mol Biol* 25:751–757. DOI: https://doi.org/10.1016/0965-1748(95)00015-n.

Blomquist GJ, Bagnères AG. 2010. Insect hydrocarbons: biology, biochemistry, and chemical ecology. Cambridge University Press, New York, USA.

Blomquist GJ, Ginzel MD. 2021. Chemical ecology, biochemistry, and molecular biology of insect hydrocarbons. *Annu Rev Entomol* 66:45–60. DOI: https://doi.org/10.1146/annurev-ento-031620-071754.

Bontonou G, Shaik HA, Denis B, Wicker-Thomas, C. 2015. Acp70A regulates *Drosophila* pheromones through juvenile hormone induction. *Insect Biochem Mol Biol* 56:36–49. DOI: https://doi.org/10.1016/j.ibmb.2014.11.008.

Bownes M, Smith T. 1984. Ecdysteroids in adult males and females of *Drosophila melanogaster*. *J Insect Physiol* 30:823–830. DOI: https://doi.org/10.1016/0022-1910(84)90019-2.

Chase J, Jurenka RA, Schal C, Halarnkar PP, Blomquist GJ. 1990. Biosynthesis of methyl branched hydrocarbons of the German cockroach *Blattella germanica* (L.) (Orthoptera, Blattellidae). *Insect*

Biochem 20:149-156. DOI: https://doi.org/10.1016/0020-1790(90)90007-H.

Chase J, Touhara K, Prestwich GD, Schal C, Blomquist GJ. 1992. Biosynthesis and endocrine control of the production of the German cockroach sex pheromone 3,11-dimethylnonacosan-2-one. *Proc Natl Acad Sci USA* 89:6050–6054. DOI: https://doi.org/10.1073/pnas.89.13.6050.

Chen N, Pei XJ, Li S, Fan YL, Liu TX. 2020. Involvement of integument-rich *CYP4G19* in hydrocarbon biosynthesis and cuticular penetration resistance in *Blattella germanica* (L.). *Pest Manag Sci* 76:215–226. DOI: https://doi.org/10.1002/ps.5499.

Chertemps T, Duportets L, Labeur C, Ueyama M, Wicker-Thomas C. 2006. A female specific desaturase gene responsible for diene hydrocarbon biosynthesis and courtship behaviour in *Drosophila melanogaster*. *Insect Mol Biol* 15:465–473. DOI: https://doi.org/10.1111/j.1365-2583.2006.00658.x.

Chertemps T, Duportets L, Labeur C, Ueda R, Takahashi K, Saigo K, Wicker-Thomas C. 2007. A female-biased expressed elongase involved in long-chain hydrocarbon biosynthesis and courtship behavior in *Drosophila melanogaster*. *Proc Natl Acad Sci USA* 104: 4273–4278. https://doi.org/10.1073/pnas.0608142104.

Chung H, Loehlin DW, Dufour HD, Vaccarro K, Millar JG, Carroll SB. 2014. A single gene affects both ecological divergence and mate choice in *Drosophila*. *Science* 343:1148–1151. DOI: https://doi.org/10.1126/science.1249998.

Chung H, Carroll SB. 2015. Wax, sex and the origin of species: Dual roles of insect cuticular hydrocarbons in adaptation and mating. *BioEssays* 37:822–830. DOI: https://doi.org/10.1002/bies.201500014.

Clough E, Jimenez E, Kim YA, Whitworth C, Neville MC, Hempel LU, Pavlou HJ, Chen ZX, Sturgill D, Dale RK, Smith HE, Przytycka TM, Goodwin SF, Van Doren M, Oliver B. 2014. Sex- and tissue-specific functions of *Drosophila* doublesex transcription factor target genes. *Dev Cell* 31:761–773. DOI: https://doi.org/10.1016/j.devcel.2014.11.021.

Connallon T, Knowles LL. 2005. Intergenomic conflict revealed by patterns of sex-biased gene expression. *Trends Genet* 21:495–499. DOI: https://doi.org/10.1016/j.tig.2005.07.006.

Darwin C. 1871. The descent of man, and selection in relation to sex. London, UK: J. Murray.

Eliyahu D, Nojima S, Mori K, Schal C. 2008a. New contact sex pheromone components of the German cockroach, *Blattella germanica*, predicted from the proposed biosynthetic pathway. *J Chem Ecol* 34:229–237. DOI: https://doi.org/10.1007/s10886-007-9409-8.

717 Eliyahu D, Nojima S, Capracotta SS, Comins DL, Schal, C. 2008b. Identification of cuticular lipids
718 eliciting interspecific courtship in the German cockroach, *Blattella germanica*. *Naturwissenschaften*
719 95:403–412. DOI: https://doi.org/10.1007/s00114-007-0339-7.
720 Eliyahu D, Nojima S, Mori K, Schal C. 2009. Jail baits: how and why nymphs mimic adult females of the
721 German cockroach, *Blattella germanica*. *Anim Behav* 78:1097–1105. DOI:
722 https://doi.org/10.1016/j.anbehav.2009.06.035.
723 Fan YL, Chase J, Sevala VL, Schal C. 2002. Lipophorin-facilitated hydrocarbon uptake by oocytes in the
724 German cockroach *Blattella germanica* (L.). *J Exp Biol* 205:781–790. DOI:
725 https://jeb.biologists.org/content/205/6/781.
726 Fan YL, Eliyahu D., Schal C. 2008. Cuticular hydrocarbons as maternal provisions in embryos and nymphs
727 of the cockroach *Blattella germanica*. *J Exp Biol* 211: 548-554. DOI:
728 https://jeb.biologists.org/content/211/4/548.
729 Fedina TY, Arbuthnott D, Rundle HD, Promislow D, Pletcher SD. 2017. Tissue-specific insulin signaling
730 mediates female sexual attractiveness. *PLoS Genet* 13:e1006935. DOI:
731 https://doi.org/10.1371/journal.pgen.1006935.
732 Ferveur JF, Sureau G. 1996. Simultaneous influence on male courtship of stimulatory and inhibitory
733 pheromones produced by live sex-mosaic *Drosophila melanogaster*. *Proc R Soc B* 263:967–973. DOI:
734 https://doi.org/10.1098/rspb.1996.0143.
735 Ferveur JF, Savarit F, O'Kane CJ, Sureau G, Greenspan RJ, Jallon JM. 1997. Genetic feminization of
736 pheromones and its behavioral consequences in *Drosophila* males. *Science* 276:1555–1558. DOI:
737 https://doi.org/10.1126/science.276.5318.1555.
738 Gempe T, Beye M. 2011. Function and evolution of sex determination mechanisms, genes and pathways in
739 insects. *BioEssays* 33:52–60. DOI: https://doi.org/10.1002/bies.201000043.
740 Gibbs AG, 1998. Water-proofing properties of cuticular lipids. *Am Zool* 38:471–482. DOI:
741 https://doi.org/10.1093/icb/38.3.471.
742 Ginzel MD, Blomquist GJ. 2016. Insect hydrocarbons: biochemistry and chemical ecology. In: Cohen, E.,
743 Moussian, B. (Eds.), Extracellular Composite Matrices in Arthropods. Springer, pp. 221–252.
744 Gu X, Quilici D, Juarez P, Blomquist GJ, Schal C. 1995. Biosynthesis of hydrocarbons and contact sex
745 pheromone and their transport by lipophorin in females of the German cockroach (*Blattella*

germanica). *J Insect Physiol* 41:257–267. DOI: https://doi.org/10.1016/0022-1910(94)00100-U.

Hall AB, Basu S, Jiang X, Qi Y, Timoshevskiy VA, Biedler JK, Sharakhova MV, Elahi R, Anderson MA, Chen XG, Sharakhov IV, Adelman ZN, Tu Z. 2015. A male-determining factor in the mosquito *Aedes aegypti*. *Science* 348:1268–1270. DOI: https://doi.org/10.1126/science.aaa2850.

Harrison MC, Jongepier E, Robertson HM, Arning N, Bitard-Feildel T, Chao H, Childers CP, Dinh, H, Doddapaneni H, Dugan S, Gowin J, Greiner C, Han Y, Hu H, Hughes DST, Huylmans AK, Kemena C, Kremer LPM, Lee SL, Lopez-Ezquerra A, Mallet L, Monroy-Kuhn JM, Moser A, Murali SC, Muzny DM, Otani S, Piulachs MD, Poelchau M, Qu J, Schaub F, Wada-Katsumata A, Worley KC, Xie Q, Ylla G, Poulsen M, Gibbs RA, Schal C, Richards S, Belles X, Korb J, Bornberg-Bauer E. 2018. Hemimetabolous genomes reveal molecular basis of termite eusociality. *Nat Ecol Evol* 2:557–566. DOI: https://doi.org/10.1038/s41559-017-0459-1.

Hasselmann M, Gempe T, Schiøtt M, Nunes-Silva CG, Otte M, Beye M. 2008. Evidence for the evolutionary nascence of a novel sex determination pathway in honeybees. *Nature* 454:519–522. DOI: https://doi.org/10.1038/nature07052.

Hastings N, Agaba M, Tocher DR, Leaver MJ, Dick JR, Sargent JR, Teale AJ. 2001. A vertebrate fatty acid desaturase with Delta 5 and Delta 6 activities. *Proc Natl Acad Sci USA* 98:14304–14309. DOI: https://doi.org/10.1073/pnas.251516598.

Herpin A, Schartl M. 2015. Plasticity of gene-regulatory networks controlling sex determination: of masters, slaves, usual suspects, newcomers, and usurpators. *EMBO Rep* 16:1260–1274. DOI: https://doi.org/10.15252/embr.201540667.

Holze H, Schrader L, Buellesbach J. 2020. Advances in deciphering the genetic basis of insect cuticular hydrocarbon biosynthesis and variation. *Heredity*: In press. DOI: https://doi.org/10.1038/s41437-020-00380-y.

Howard RW, Blomquist GJ. 2005. Ecological, behavioral, and biochemical aspects of insect hydrocarbons. *Annu Rev Entomol* 50:371–393. DOI: https://doi.org/10.1146/annurev.ento.50.071803.130359.

Ingleby FC, Innocenti P, Rundle HD, Morrow EH. 2014. Between-sex genetic covariance constrains the evolution of sexual dimorphism in *Drosophila melanogaster*. *J Evol Biol* 27:1721–1732. DOI: https://doi.org/10.1111/jeb.12429.

Innocenti P, Morrow EH. 2010. The sexually antagonistic genes of *Drosophila melanogaster*. *PLoS Biol*

775 8:e1000335. DOI: https://doi.org/10.1371/journal.pbio.1000335.

776 Juárez MP, Chase J, Blomquist GJ. 1992. A microsomal fatty acid synthetase from the integument of
777 *Blattella germanica* synthesizes methyl-branched fatty acids, precursors to hydrocarbon and contact
778 sex pheromone. *Arch Insect Biochem Physiol* 293:333–341. DOI: https://doi.org/10.1016/0003-
779 9861(92)90403-j.

780 Juárez MP, Ayala S, Brenner RR. 1996. Methyl-branched fatty acid biosynthesis in *Triatoma infestans*.
781 *Insect Biochem Mol Biol* 26:599–605. DOI: https://doi.org/10.1016/S0965-1748(96)00021-5.

782 Juárez MP. 2004. Fatty acyl-CoA elongation in *Blatella germanica* integumental microsomes. *Arch Insect*
783 *Biochem Physiol* 56: 170–178. DOI: https://doi.org/10.1002/arch.20007.

784 Jurenka RA, Schal C, Burns E, Chase J, Blomquist GJ. 1989. Structural correlation between cuticular
785 hydrocarbons and female contact sex pheromone of German cockroach *Blattella germanica* (L.). *J*
786 *Chem Ecol* 15:939–949. DOI: https://doi.org/10.1007/BF01015189.

787 Kiuchi T, Koga H, Kawamoto M, Shoji K, Sakai H, Arai Y, Ishihara G, Kawaoka S, Sugano S, Shimada T,
788 Suzuki Y, Suzuki MG, Katsuma S. 2014. A single female-specific piRNA is the primary determiner of
789 sex in the silkworm. *Nature* 509:633–636. https://doi.org/10.1038/nature13315.

790 Kopp A. 2012. *Dmrt* genes in the development and evolution of sexual dimorphism. *Trends Genet* 28:175–
791 184. DOI: https://doi.org/10.1016/j.tig.2012.02.002.

792 Kunte K. 2008. Mimetic butterflies support Wallace's model of sexual dimorphism. *Proc R Soc B*
793 275:1617–1624. DOI: https://doi.org/10.1098/rspb.2008.0171.

794 Kuo TH, Fedina TY, Hansen I, Dreisewerd K, Dierick HA, Yew JY, Pletcher S.D. 2012. Insulin signaling
795 mediates sexual attractiveness in *Drosophila*. *PLoS Genet* 8:e1002684. DOI:
796 https://doi.org/10.1371/journal.pgen.1002684.

797 Lepage G, Roy C. 1984. Improved recovery of fatty acid through direct transesterification without prior
798 extraction or purification. *J Lipid Res* 25:1391–1396.

799 Legendre A, Miao XX, Da Lage JL, Wicker-Thomas C. 2008. Evolution of a desaturase involved in female
800 pheromonal cuticular hydrocarbon biosynthesis and courtship behavior in *Drosophila*. *Insect Biochem*
801 *Mol Biol* 38:244–255. DOI: https://doi.org/10.1016/j.ibmb.2007.11.005.

802 Li DT, Chen X, Wang XQ, Zhang CX. 2019a. *FAR* gene enables the brown planthopper to walk and jump
803 on water in paddy field. *Sci China Life Sci* 62:1521–1531. DOI: https://doi.org/10.1007/s11427-018-

9462-4.

Li DT, Chen X, Wang XQ, Moussian, B, Zhang CX. 2019b. The fatty acid elongase gene family in the brown planthopper, *Nilaparvata lugens*. *Insect Biochem Mol Biol* 108:32–43. DOI: https://doi.org/10.1016/j.ibmb.2019.03.005.

Livak KJ, Schmittgen TD, 2001. Analysis of relative gene expression data using real-time quantitative PCR and the 2(-Delta Delta C(T)) method. *Methods* 25:402–408. DOI: https://doi.org/10.1006/meth.2001.1262.

Lozano J, Belles X. 2011. Conserved repressive function of Krüppel homolog 1 on insect metamorphosis in hemimetabolous and holometabolous species. *Sci Rep* 1:163. https://doi.org/10.1038/srep00163.

MacLean M, Nadeau J, Gurnea T, Tittiger C, Blomquist GJ. 2018. Mountain pine beetle (*Dendroctonus ponderosae*) *CYP4Gs* convert long and short chain alcohols and aldehydes to hydrocarbons. *Insect Biochem Mol Biol* 102:11–20. DOI: https://doi.org/10.1016/j.ibmb.2018.09.005.

Mank JE. 2017. The transcriptional architecture of phenotypic dimorphism. *Nature Ecol Evol* 1:6. DOI: https://doi.org/10.1038/s41559-016-0006.

Marican C, Duportets L, Birman S, Jallon JM. 2004. Female-specific regulation of cuticular hydrocarbon biosynthesis by dopamine in *Drosophila melanogaster*. *Insect Biochem Mol Biol* 34:823–830. DOI: https://doi.org/10.1016/j.ibmb.2004.05.002.

Moon YA, Shah NA, Mohapatra S, Warrington JA, Horton JD. 2001. Identification of a mammalian long chain fatty acyl elongase regulated by sterol regulatory element-binding proteins. *J Biol Chem* 276:45358–45366. DOI: https://doi.org/10.1074/jbc.M108413200.

Nojima S, Nishida R, Kuwahara Y, Sakuma M. 1999. Nuptial feeding stimulants: a male courtship pheromone of the German cockroach, *Blattella germanica* (L.) (Dictyoptera: Blattellidae). *Naturwissenschaften* 86:193-196. DOI: https://doi.org/10.1007/s001140050596.

Oh, CS, Toke DA, Mandala S, Martin CE. 1997. *ELO2* and *ELO3*, Homologues of the *Saccharomyces cerevisiae ELO1* gene, function in fatty acid elongation and are required for sphingolipid formation. *J Boil Chem* 272:17376–17384. DOI: https://doi.org/10.1074/jbc.272.28.17376.

Ohno Y, Suto S, Yamanaka M, Mizutani Y, Mitsutake S, Igarashi Y, Sassa T, Kihara A. 2010. ELOVL1 production of C24 acyl-CoAs is linked to C24 sphingolipid synthesis. *Proc Natl Acad Sci USA* 107:18439–18444. DOI: https://doi.org/10.1073/pnas.1005572107.

833 Parvy JP, Napal L, Rubin T, Poidevin M, Perrin L, Wicker-Thomas C, Montagne J. 2012. *Drosophila*
834 *melanogaster* Acetyl-CoA-carboxylase sustains a fatty acid-dependent remote signal to waterproof the
835 respiratory system. *PLoS Genets* 8:e1002925. DOI: https://doi.org/10.1371/journal.pgen.1002925.
836 Pei XJ, Chen N, Bai Y, Qiao JW, Li S, Fan YL, Liu TX. 2019. *BgFas1*: A fatty acid synthase gene required
837 for both hydrocarbon and cuticular fatty acid biosynthesis in the German cockroach, *Blattella*
838 *germanica* (L.). *Insect Biochem Mol Biol* 112:103203. DOI:
839 https://doi.org/10.1016/j.ibmb.2019.103203.
840 Pfannenstiel RS, Booth W, Vargo EL, Schal C. 2008. *Blattella asahinai* (Dictyoptera: Blattellidae): A new
841 predator of lepidopteran eggs in south Texas soybean. *Ann Entomol Soc Am* 101:763–768.
842 Prakash A, Monteiro A. 2016. Molecular mechanisms of secondary sexual trait development in insects.
843 *Curr Opin Insect Sci* 17:40–48. DOI: https://doi.org/10.1016/j.cois.2016.06.003.
844 Qiu Y, Tittiger C, Wicker-thomas C, Goff LG, Young S, Wajnberg E, Fricaux T, Taquet N, Blomquist GJ,
845 Feyereisen R. 2012. An insect-specific p450 oxidative decarbonylase for cuticular hydrocarbon
846 biosynthesis. *Proc Natl Acad Sci USA* 109:14858–14863. DOI:
847 https://doi.org/10.1073/pnas.1208650109.
848 Rogers TF, Palmer DH, Wright AE. 2020. Sex-specific selection drives the evolution of alternative splicing
849 in birds. *Mol Biol Evol*: In press. DOI: https://doi.org/10.1093/molbev/msaa242.
850 Romaá I, Pascual, N, X. Bellés. 1995. The ovary is a source of circulating ecdysteroids in *Blattella*
851 *germanica* (Dictyoptera: Blattellidae). *Eur J Entomol* 92:93-103.
852 Schal C, Burns EL, Jurenka RA, Blomquist GJ. 1990. A new component of the female sex pheromone of
853 *Blattella germanica* (L.) (Dictyoptera: Blattellidae) and interaction with other pheromone components.
854 *J Chem Ecol* 16:1997–2008. DOI: https://doi.org/10.1007/BF01020511.
855 Schal C, Gu X, Burns EL, Blomquist GJ. 1994. Patterns of biosynthesis and accumulation of hydrocarbons
856 and contact sex pheromone in the female German cockroach, *Blattella germanica*. *Arch Insect*
857 *Biochem Physiol* 25:375–391. DOI: https://doi.org/10.1002/arch.940250411.
858 Schal C, Chiang AS. 1995. Hormonal control of sexual receptivity in cockroaches. *Experientia* 51:994–
859 998. DOI: https://doi.org/10.1007/BF01921755.
860 Schal C, Sevala V, Cardé RT. 1998. Novel and highly specific transport of a volatile sex pheromone by
861 hemolymph lipophorin in moths. *Naturwissenschaften* 85: 339–342. DOI:

https://doi:10.1007/s001140050511.

Schal C, Sevala V, Capurro ML, Snyder TE, Blomquist GJ, Bagnères AG. 2001. Tissue distribution and lipophorin transport of hydrocarbons and sex pheromones in the house fly, *Musca domestica*. *J Insect Sci* 1:12.

Schal C. 2011. Cockroaches. In Hedges S, Moreland D, editors, Handbook of Pest Control, chapter 2, pages 150–291. Pennsylvania State University: GIEMedia.

Shirangi TR, Dufour HD, Williams TM, Carroll SB. 2009. Rapid evolution of sex pheromone-producing enzyme expression in *Drosophila*. *PLoS Biol* 7:e1000168. DOI: https://doi.org/10.1371/journal.pbio.1000168.

Tanaka K, Barmina O, Sanders LE, Arbeitman MN, Kopp A. 2011. Evolution of sex-specific traits through changes in HOX-dependent *doublesex* expression. *PLoS Biol* 9:e1001131. DOI: https://doi.org/10.1371/journal.pbio.1001131.

Toke DA, Martin CE. 1996. Isolation and characterization of gene affecting fatty acid elongation in *Saccharomyces cerevisiae*. *J Biol Chem* 271:18413–18422. DOI: https://doi.org/10.1074/jbc.271.31.18413.

Verhulst EC, van de Zande L.2015. Double nexus–*Doublesex* is the connecting element in sex determination. *Brief Funct Genomics* 14:396–406. DOI: https://doi.org/10.1093/bfgp/elv005.

Wada-Katsumata A Schal, C. 2019. Antennal grooming facilitates courtship performance in a group-living insect, the German cockroach *Blattella germanica*. *Sci Rep* 9:2942. DOI: https://doi.org/10.1038/s41598-019-39868-x.

Wexler J, Delaney EK, Belles X, Schal C, Wada-Katsumata A, Amicucci MJ, Kopp A. 2019. Hemimetabolous insects elucidate the origin of sexual development via alternative splicing. *eLife* 8:e47490. DOI: https://doi.org/10.7554/eLife.47490.

Wicker C, Jallon JM. 1995a. Hormonal control of sex pheromone biosynthesis in *Drosophila melanogaster*. *J Insect Physiol* 41:65–70. DOI: https://doi.org/10.1016/0022-1910(94)00074-Q.

Wicker C, Jallon JM. 1995b. Influence of ovary and ecdysteroids on pheromone biosynthesis in *Drosophila melanogaster* (Diptera: Drosophilidae). *Eur J Entomol* 92:197202.

Wicker-Thomas C, Garrido D, Bontonou G, Napal L, Mazuras N, Denis B. Rubin T, Parvy JP, Montagne J. 2015. Flexible origin of hydrocarbon/pheromone precursors in *Drosophila melanogaster*. *J Lipid Res*

891 56:2094–2101. DOI: https://doi.org/10.1194/jlr.M060368.

892 Williams TM, Selegue JE, Werner T, Gompel N, Kopp A, Carroll SB. 2008. The regulation and evolution
893 of a genetic switch controlling sexually dimorphic traits in *Drosophila*. *Cell* 134:610–623. DOI:
894 https://doi.org/10.1016/j.cell.2008.06.052.

895 Yew JY, Chung H. 2015. Insect pheromones: An overview of function, form, and discovery. *Prog Lipid Res*
896 59:88–105. DOI: https://doi.org/10.1016/j.plipres.2015.06.001.

897 Young HP, Larabee JK, Gibbs AG, Schal C. 2000. Relationship between tissue-specific hydrocarbon
898 profiles and lipid melting temperatures in the cockroach *Blattella germanica*. *J Chem Ecol* 26:1245-
899 1263. DOI: https://doi.org/10.1023/A:1005440212538.

900 Zhang Z, Klein J, Nei M. 2014a. Evolution of the *sex-lethal* gene in insects and origin of the sex-
901 determination system in *Drosophila*. *J Mol Evol* 78:50–65. DOI: https://doi.org/10.1007/s00239-013-
902 9599-3.

903 Zhang B, Xue HJ, Song KQ, Liu J, Li WZ, Nie RE, Yang XK. 2014b. Male mate recognition via cuticular
904 hydrocarbons facilitates sexual isolation between sympatric leaf beetle sister species. *J Insect Physiol*
905 70:15–21. DOI: https://doi.org/10.1016/j.jinsphys.2014.08.006.

906 Zhao X, Yang Y, Niu N, Zhao Y, Zhang J. 2020. The fatty acid elongase gene *LmElo7* is required for
907 hydrocarbon biosynthesis and cuticle permeability in the migratory locust, *Locusta migratoria*. *J*
908 *Insect Physiol* 123: 104052. DOI: https://doi.org/10.1016/j.jinsphys.2020.104052.

909 Zinna RA, Gotoh H, Kojima T, Niimi T. 2018. Recent advances in understanding the mechanisms of
910 sexually dimorphic plasticity: insights from beetle weapons and future directions. *Curr Opin Insect Sci*
911 25:35–41. DOI: https://doi.org/10.1016/j.cois.2017.11.009.

912

Figures and figure legends

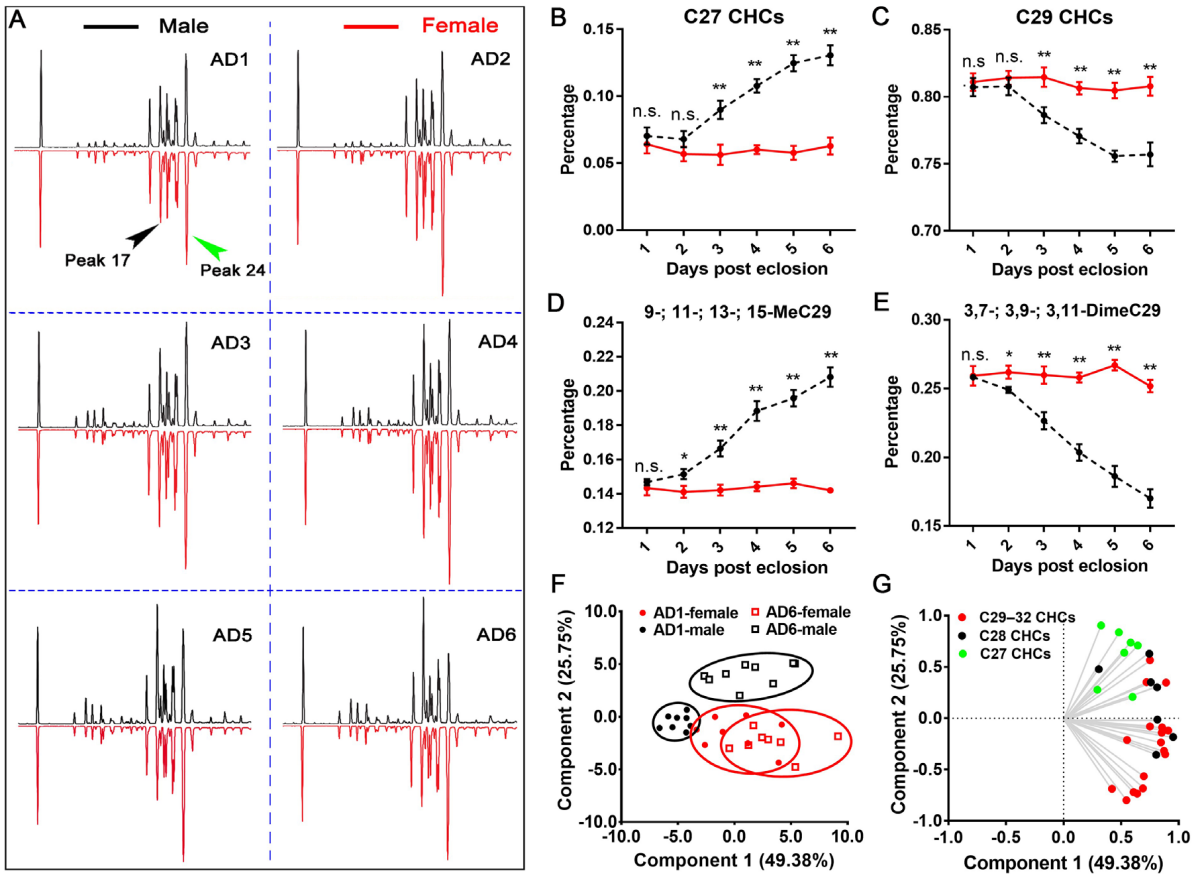

Figure 1. Development of sexually dimorphic cuticular hydrocarbons. **(A)** Comparisons of 1- to 6-day-old adult (AD1–AD6) male (black) and female (red) cuticular hydrocarbon profiles. The first peak represents the internal standard *n*-hexacosane. Other peaks correspond to the CHCs in Source data 1. Peak 17 is male-enriched (9-; 11-; 13-; 15-MeC29) and gradually increased with age in males. Peak 24 is female-enriched (3,7-; 3,9-; 3,11-DimeC29). The proportions of C27 CHCs **(B)**, C29 CHCs **(C)**, Peak 17 **(D)**, and Peak 24 **(E)** in the total CHCs from AD1 to AD6 were compared between males (black dotted lines) and females (solid red lines). Data are shown as mean ± SEM (n.s. represent no significant difference; $*P < 0.05$, $**P < 0.01$, two-tailed Student's *t*-test, n = 8–10). **(F, G)** Principal component analysis of AD1 and AD6 CHC profiles of males and females. In **(F)**, each dot represents a datum calculated from one cockroach. AD1 male (black solid circles) and female (red solid circles) CHC profiles overlapped, whereas AD6 male (black open square) and female (red open square) CHC profiles separated along PC2. In the loading diagram **(G)**, CHCs with different chain lengths are marked by green (C27), black (C28), and red (C29–C32), showing that C27 CHCs vectored toward males along PC2, whereas longer chain CHCs vectored toward females.

The following Source data and figure supplements are available for figure 1:

930 **Source data 1.** Quantification of different cuticular hydrocarbons during sexually dimorphic cuticular

931 hydrocarbon generation.

932 **Figure 1–figure supplement 1.** Cuticular hydrocarbon profiles of 4-day-old sixth-instar nymphs of *Blattella*

933 *Germanica*.

934

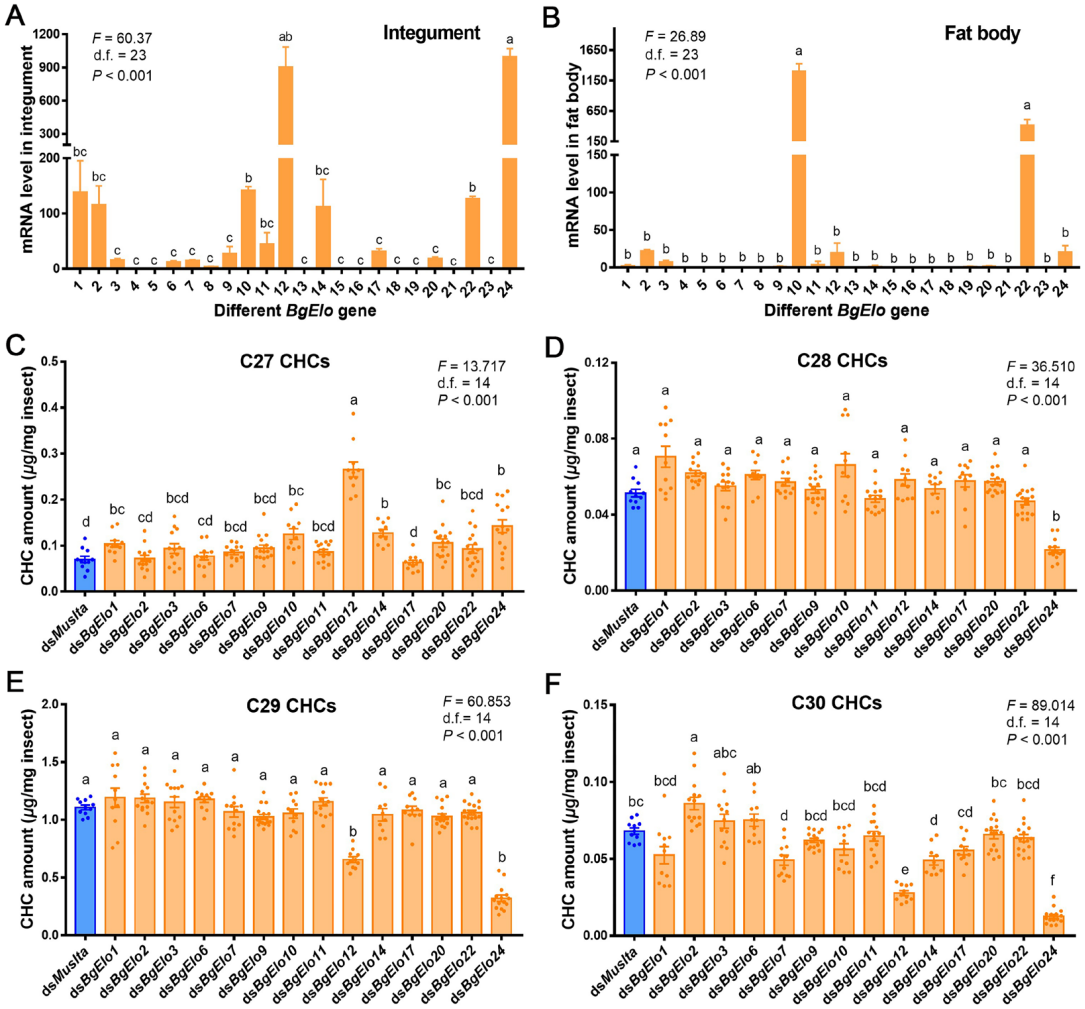

Figure 2. RNAi screen to identify *BgElo* genes involved in long-chain cuticular hydrocarbon biosynthesis. Transcript levels of different *BgElo* genes in the abdominal integument **(A)** and fat body **(B)**. The numbers on the abscissa correspond to *BgElo1–24*. Data are shown as mean ± SEM, and calculated from 4 replicates (each replicate contains 4 cockroaches for the integument and 8 cockroaches for the fat body). The influence of knockdown of different *BgElo* genes on C27 **(C)**, C28 **(D)**, C29 **(E)**, C30, and **(F)** CHCs is shown. Data are presented as mean ± SEM and calculated from 10–16 AD2 female cockroaches, each dot indicating a single datum from one cockroach. Only RNAi of *BgElo12* and *BgElo24* resulted in significant increases of C27 CHCs and decreases of C29 CHCs. Different letters indicate statistically significant differences between groups using Welch's ANOVA (Games-Howell multiple comparisons test, $P < 0.05$).

The following Source data and figure supplements are available for figure 2:

Source data 2. Quantification of individual cuticular hydrocarbons after RNAi of other *BgElo* genes.

Figure 2–figure supplement 1. RNAi efficiency of different *BgElo* genes in *Blattella germanica*.

949 **Figure 2–figure supplement 2.** Influence of *BgElo*-RNAi on cuticular hydrocarbons with chain length longer

950 than 30 carbons.

951

952

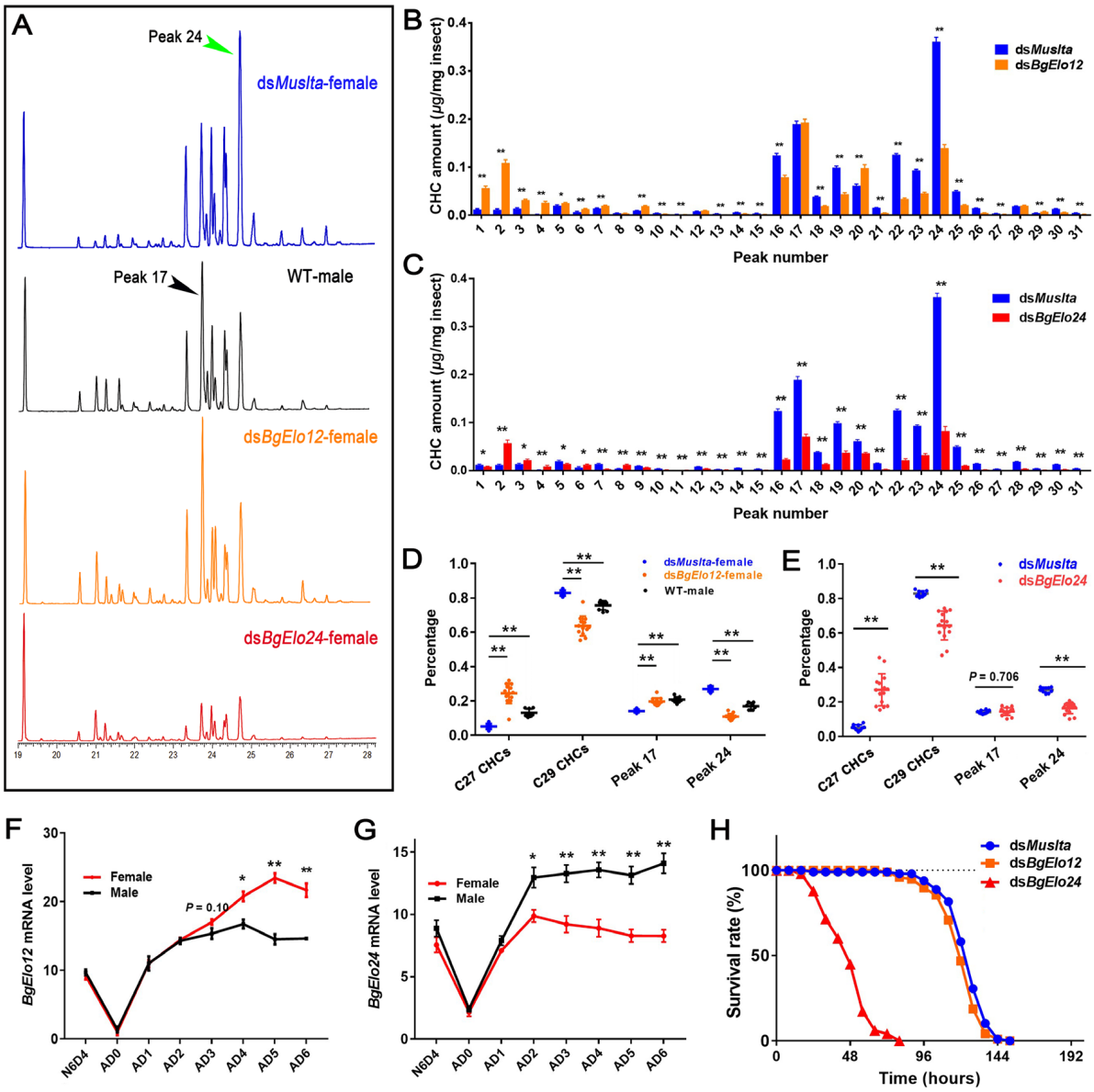

Figure 3. *BgElo12* is involved in generating sexually dimorphic hydrocarbons. **(A)** Gas chromatogram of CHC profiles from differently treated cockroaches. The CHC profiles of sexually mature females and males (AD6–AD8) showed a marked difference, and RNAi of only *BgElo12* in females generated a male-like CHC profile. Quantitative influence of *BgElo12*-RNAi **(B)** and *BgElo24*-RNAi **(C)** in females on the amount of each CHC. Percentage change of the C27 CHCs, C29 CHCs, male-enriched peak 17, and female-enriched peak 24 after *BgElo12*-RNAi **(D)** or *BgElo24*-RNAi **(E)**. Data in **(B–E)** are shown as mean ± SEM, $*P < 0.05$, $**P < 0.01$; two-tailed Student's *t*-test, n = 10 for *dsMuslta*, 11 for *dsBgElo12*, and 15 for *dsBgElo24*, 9 for wild type males (WT-male). Relative expression of *BgElo12* **(F)** and *BgElo24* **(G)** among different developmental stages and different ages of adult males and females. *P* values were calculated from 4 replicates (2–3 cockroaches/replicate), $**P < 0.01$; two-tailed Student's *t*-test. **(H)** Survival rates of *dsMuslta* (n = 98),

964 *dsBgElo12* (n = 96), and *dsBgElo24* (n = 98) treated female cockroaches maintained at 5% RH. Survival rates
965 were calculated every 8 h until all cockroaches died.
966
967 The following figure supplements are available for figure 3:
968 **Figure 3–figure supplement.** Influence of *BgElo12*-RNAi and *BgElo24*-RNAi on CHC profiles of male *B.*
969 *germanica*.
970 **Figure 3–figure supplement 2.** Verifying the influences of *BgElo12* and *BgElo24* on hydrocarbon biosynthesis
971 by using the second RNAi targets and examining changes of internal hydrocarbons.
972 **Figure 3–figure supplement 3.** Tissue-specific expression of *BgElo12* and *BgElo24*.
973
974

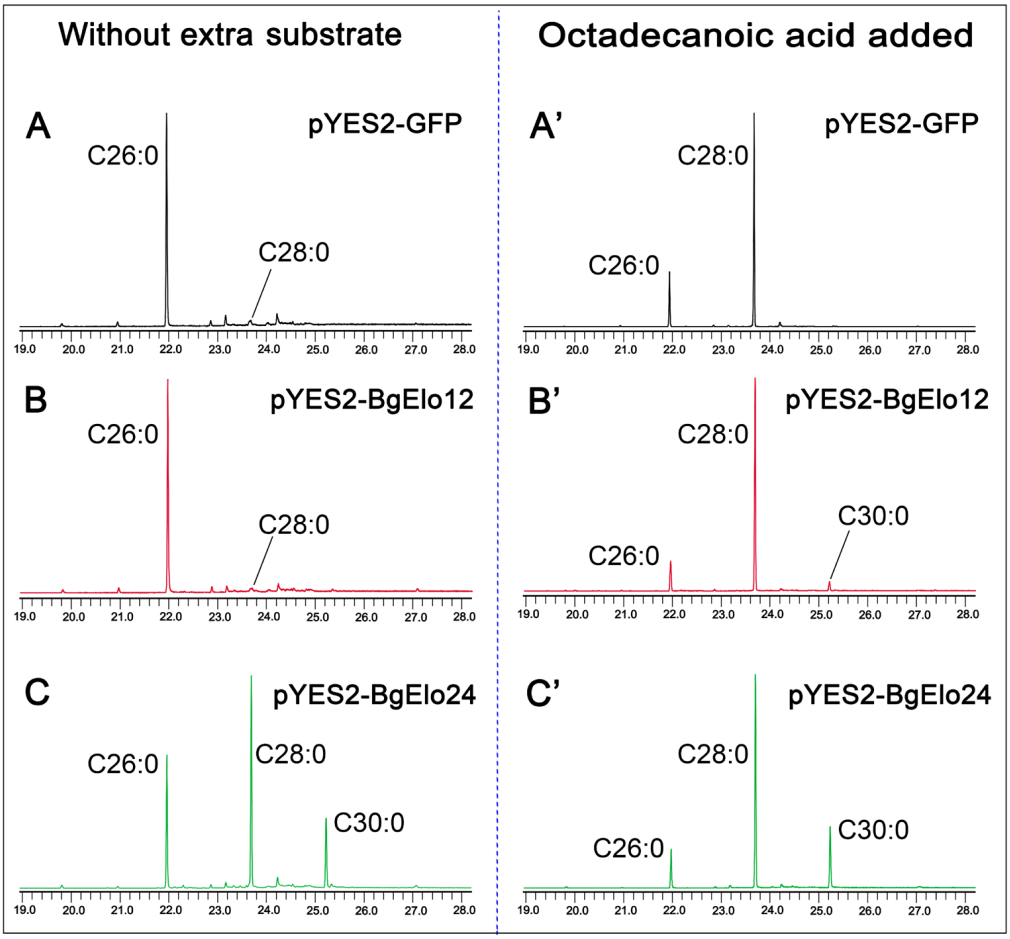

Figure 4. Yeast expression and substrate catalysis of BgElo12 and BgElo24. Representative gas chromatogram of fatty acid methyl esters of yeast transformed with pYES2-GFP **(A)**, pYES2-BgElo12 **(B)**, and pYES2-BgElo24 **(C)** without adding of extra substrates. After adding octacosanoic acid (C28:0), the corresponding chromatograms are shown at the right for pYES2-GFP **(A')**, pYES2-BgElo12 **(B')**, and pYES2-BgElo24 **(C')**. The chromatograms are truncated, and only chromatographic peaks of interest are indicated. The FAMEs are labeled by their corresponding saturated FAs. Complete chromatograms are shown in Figure 4–supplement figure 1.

The following source data and figure supplements are available for figure 4:

Source data 3. Calculation of the proportions of different fatty acid methyl esters in the yeast expression.

Figure 4–figure supplement 1. Heterologous expression of BgElo12 and BgElo24 with methyl-branched substrates.

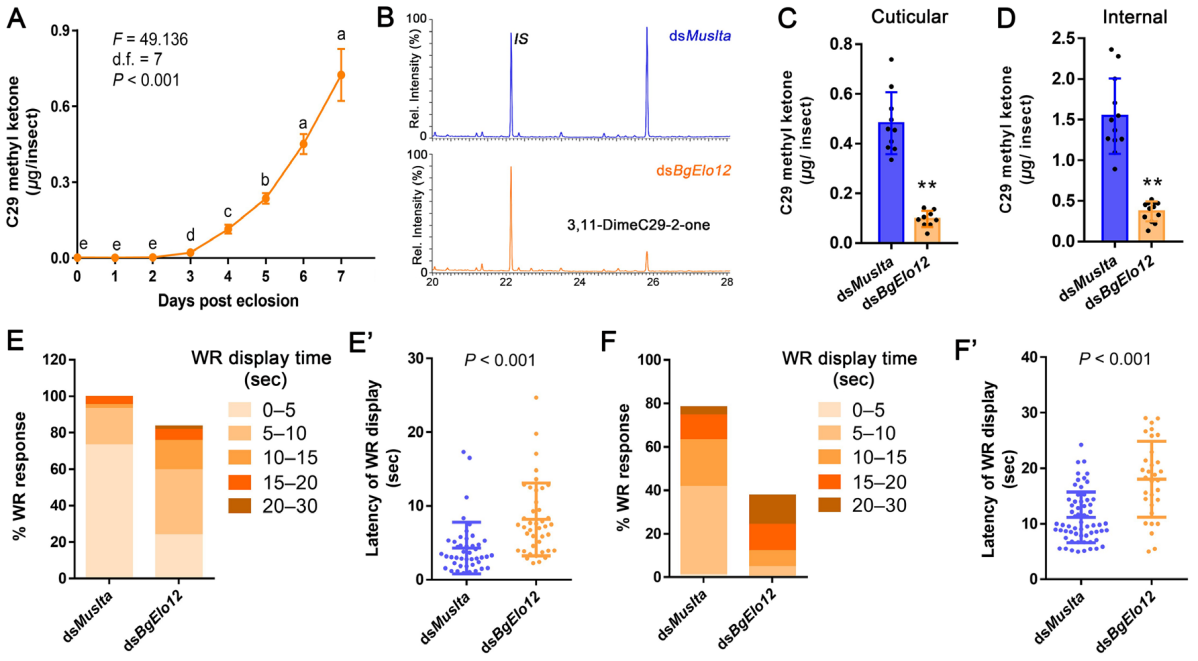

Figure 5. *BgElo12*-RNAi effects on contact sex pheromone biosynthesis in females and male courtship performance. **(A)** The pattern of contact sex pheromone (3,11-DimeC29-2-one) accumulation during female sexual maturation. Data are shown as mean ± SEM. Different letters indicate significant differences between groups using Welch's ANOVA (Games-Howell multiple comparisons test, $P < 0.05$). **(B)** Representative chromatogram showing lower amounts of sex pheromone after *BgElo12*-RNAi. *IS* is the internal standard 14-heptacosanone. Cuticular **(C)** and internal **(D)** amounts of 3,11-DimeC29-2-one (C29 methyl ketone) after *BgElo12*-RNAi. Data are shown as mean ± SD, and each replicate is shown as a dot. $^{**}P < 0.01$, two-tailed Student's *t*-test; n = 9–12. Influence of *BgElo12*-RNAi on the ability of AD5 **(E–E')** and AD3 **(F–F')** female antennae to elicit courtship in males. The percentage of males that responded with a wing-raising (WR) behavior in response to contact with female antenna were determined for 44 (*dsMuslta*) and 49 (ds*BgElo12*) female antennae in **(E)**, and 79 (ds*Muslta*) and 82 (ds*BgElo12*) antennae in **(F)**. Each female antenna was tested only once with a single male. The proportion of WR display over different time periods is shown in progressively darker colors. **(E')** and **(F')** Average latency of WR display calculated from those antennae that successfully activated a courtship behavior of males within 30 s. Data are shown as mean ± SD, each dot represents a datum calculated from one antenna. *P* values were determined by two-tailed Student's *t*-test.

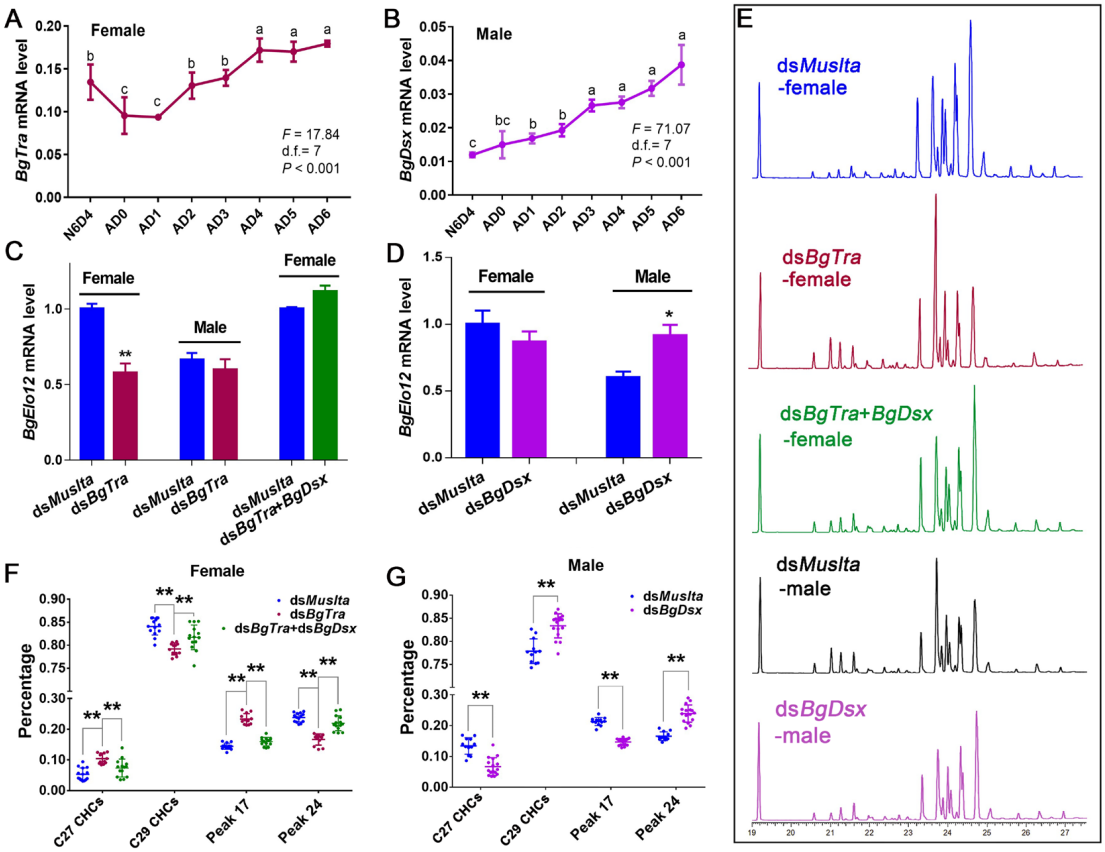

Figure 6. Regulation of *BgElo12* and sexually dimorphic hydrocarbon profiles by sex-differentiation genes. Temporal patterns of *BgTra* expression in females **(A)** and *BgDsx* expression in males **(B)**. Data are shown as mean ± SEM and calculated from 4 replicates (2–3 cockroaches/replicate). N6D4 is 6th instar nymph on day 4, AD0–6 represent adult days 0 to 6. Different letters indicate significant differences between the groups (ANOVA, Fisher's LSD, $P < 0.05$). **(C)** and **(D)** Regulation of *BgElo12* expression by *BgTra* and *BgDsx*. Data are shown as mean calculated from 4 replicates (2–3 cockroaches/replicate) ± SEM; *$P < 0.05$, **$P < 0.01$, two-tailed Student's *t*-test. **(E)** Gas chromatograms of CHCs after repressing different sex-differentiation genes. **(F)** Regulation of the proportions of representative CHCs by *BgTra* in females. Data are presented as mean ± SD, **$P < 0.01$; two-tailed Student's *t*-test; n = 14 for *dsMuslta*, 12 for ds*BgTra*, and 14 for ds*BgTra*+ds*BgDsx*. **(G)** The proportion change of representative CHCs after *BgDsx*-RNAi in males. Data are shown as mean ± SD; **$P < 0.01$; two-tailed Student's *t*-test, n = 12 for *dsMuslta* and 16 for ds*BgDsx*.

The following figure supplements are available for figure 6:

Figure 6–figure supplement 1. Verifying the sex-specific developmental function of *BgTra* and *BgDsx*.

Figure 6–figure supplement 2. Transcriptional activity of *BgDsx*^{M} on the upstream regulatory sequence of *BgElo12*.

Figure 6–figure supplement 3. Influence of *BgDsx*-RNAi and *BgTra*-RNAi on *BgElo24* expression.

Figure 6–figure supplement 4. Regulation of cuticular hrdrocarbon profiles by sex-differentiation genes.

Figure 6–figure supplement 5. Regulation of internal hydrocarbon profiles by sex-differentiation genes.

Figure 6–figure supplement 6. Regulation of *Krh1* by *BgTra* in females.

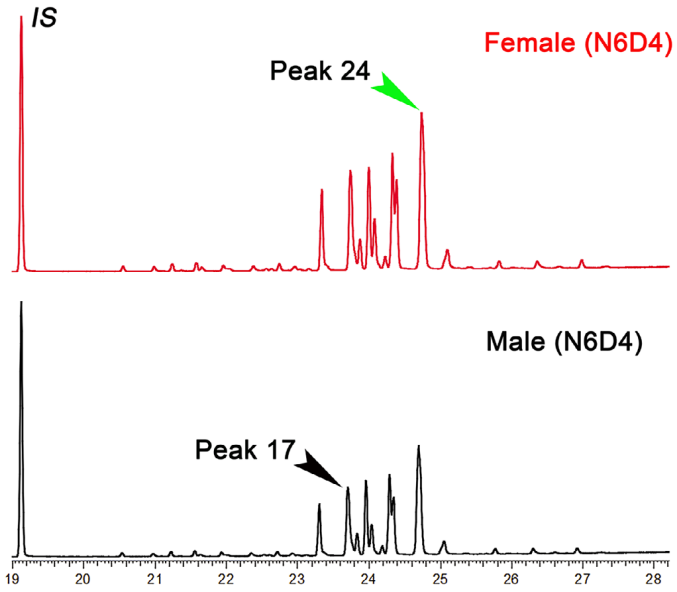

Figure 1–figure supplement 1. Cuticular hydrocarbon profiles of 4-day-old sixth-instar nymphs of *Blattella germanica*. Peak 24 represents the female-enriched 3,7-; 3,9-; 3,11-DimeC29, and Peak 17 is the male-enriched 9-; 11-; 13-; 15-MeC29.

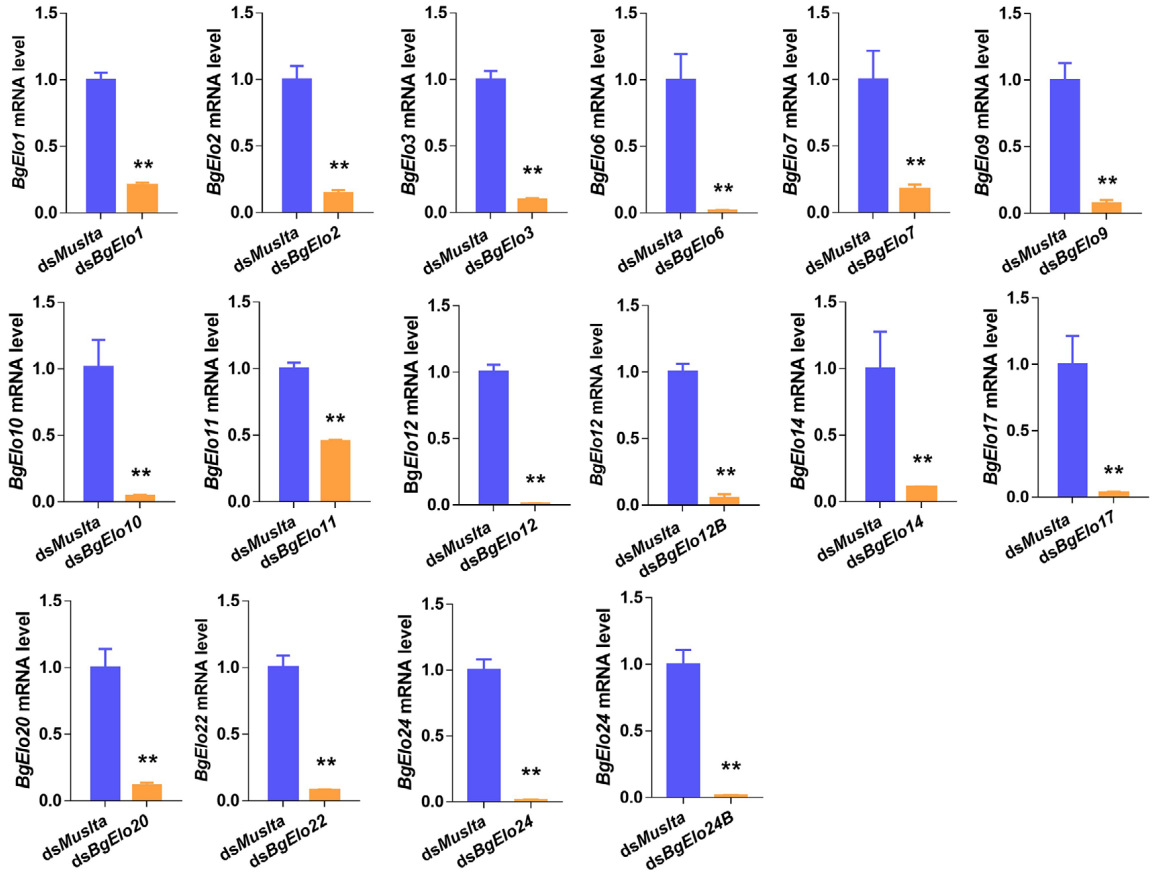

Figure 2–figure supplement 1. RNAi efficiency of different *BgElo* genes in *Blattella germanica*. Data are shown as mean ± SEM, calculated from 4 replicates (2–3 cockroaches/replicate); $^{**}P < 0.01$, two-tailed Student's *t*-test.

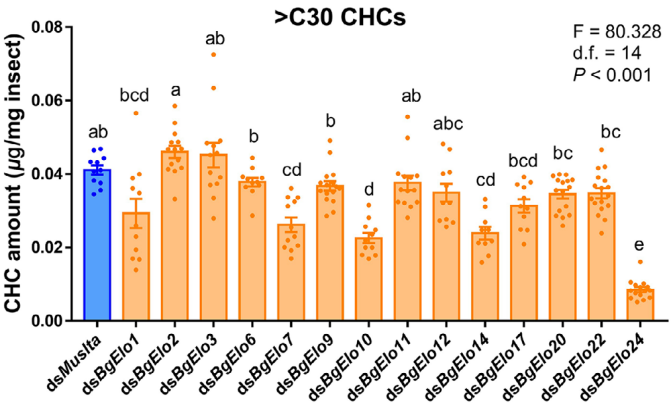

1039

1040 **Figure 2–figure supplement 2.** Effects of *BgElo*-RNAi on cuticular hydrocarbons of *Blattella germanica* with

1041 chain length longer than 30. Different letters indicate significant differences between groups using Welch's

1042 ANOVA (Games-Howell multiple comparisons test, $P < 0.05$).

1043

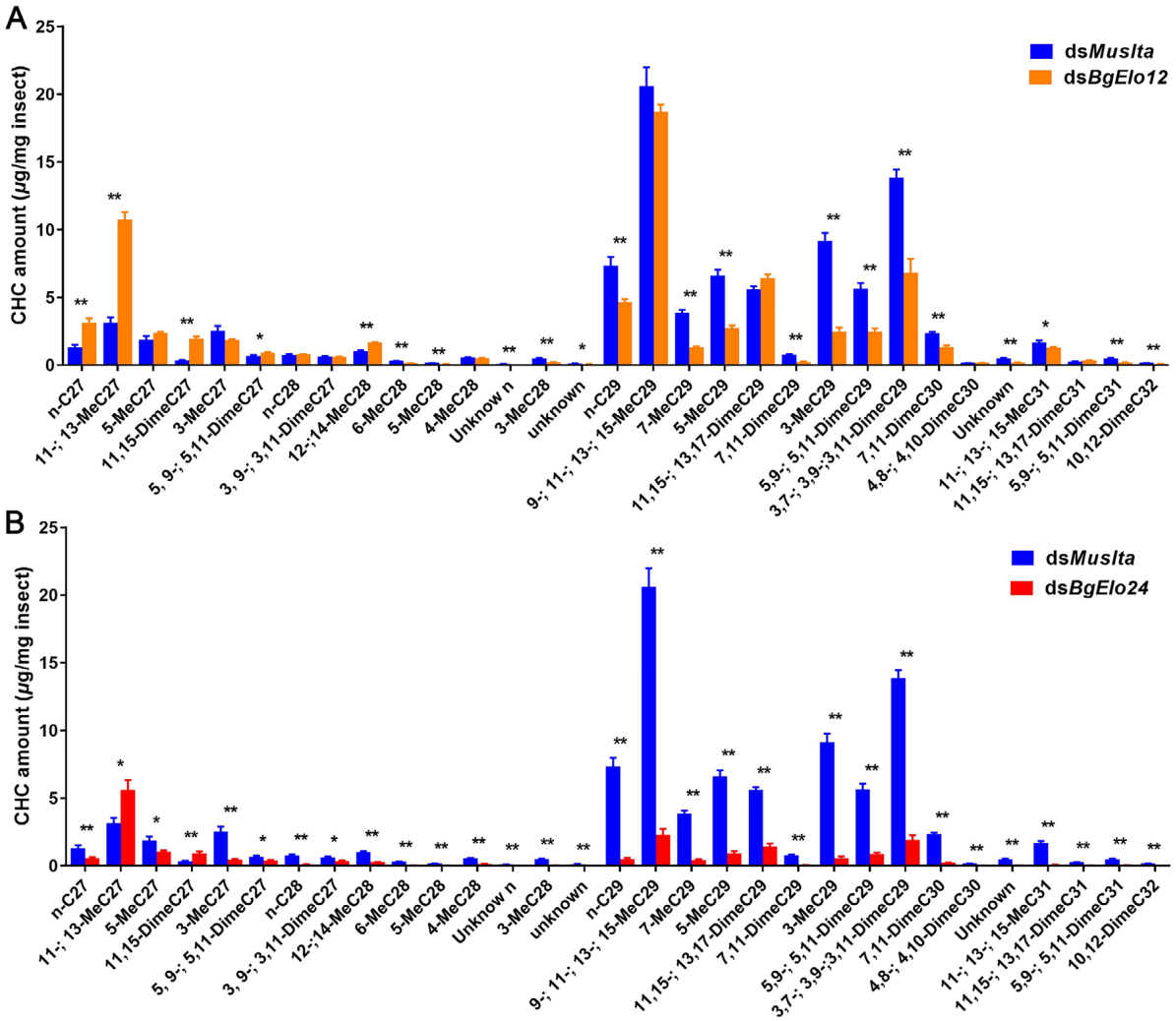

Figure 3–figure supplement 1. Effects of *BgElo12*-RNAi and *BgElo24*-RNAi on CHC profiles of male *B. germanica*. Data are shown as mean ± SEM; **P* < 0.05, ***P* < 0.01; two-tailed Student's *t*-test, n = 9 or 10.

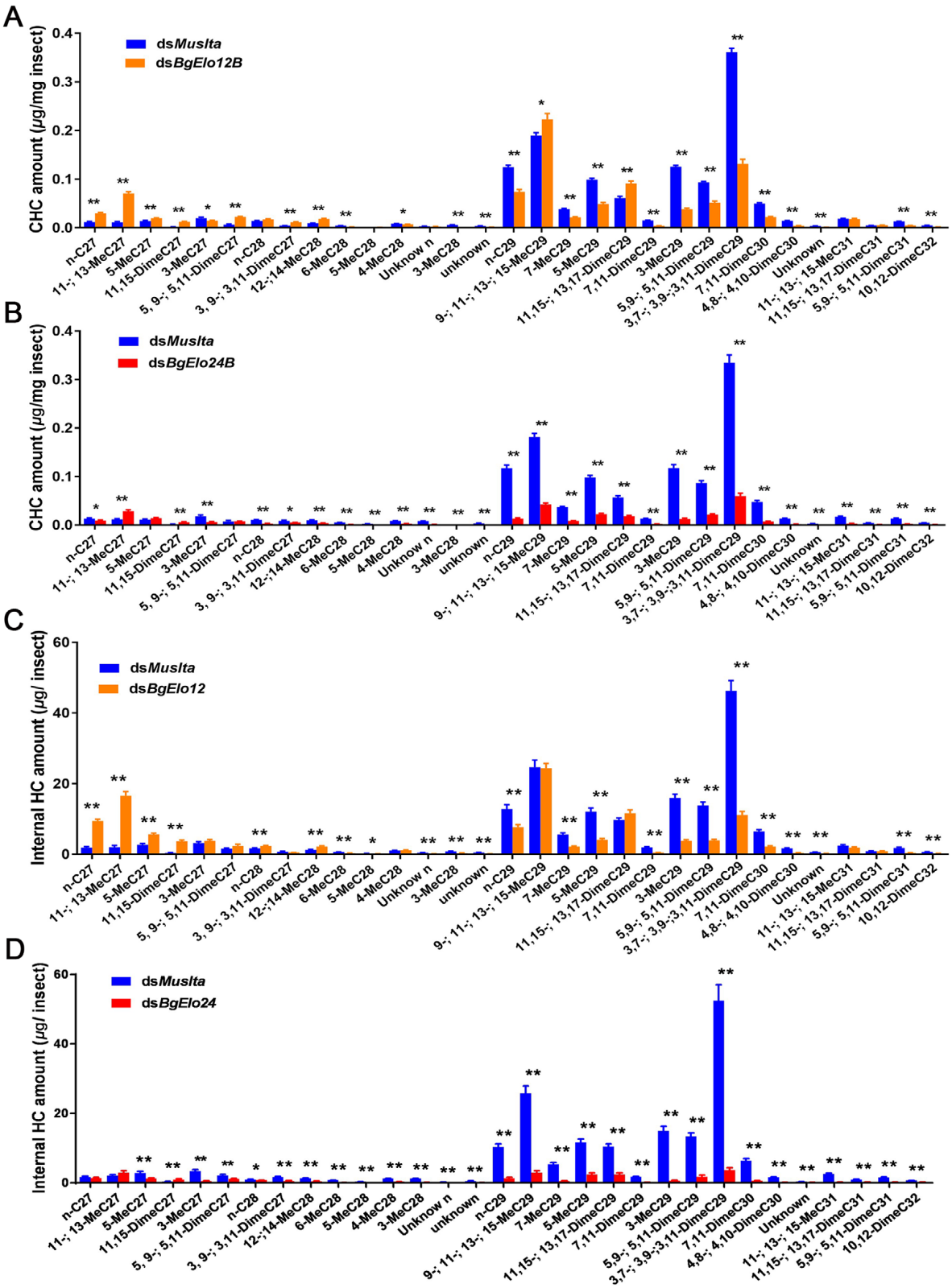

Figure 3–figure supplement 2. Verifying the roles of *BgElo12* and *BgElo24* in hydrocarbon biosynthesis by the second RNAi targets. **(A)** Analysis of cuticular hydrocarbons after RNAi of *BgElo12* using the second target (ds*BgElo12B*), **(B)** or after RNAi of *BgElo24* using the second target (ds*BgElo24B*). **(C)** and **(D)** The effects of

1051 *BgElo12*-RNAi and *BgElo24*-RNAi on internal hydrocarbons. Data are shown as mean ± SEM; **P* < 0.05, ***P* <

1052 0.01; two-tailed Student's *t*-test, n = 10–12.

1053

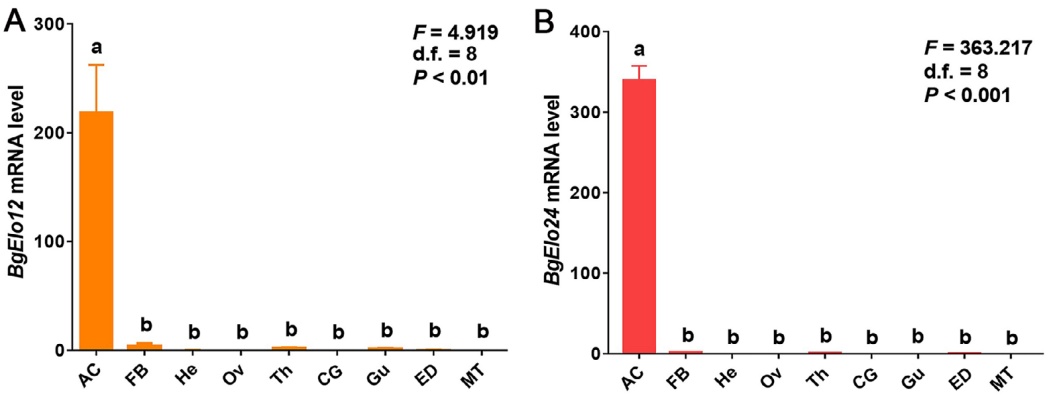

Figure 3–figure supplement 3. Tissue-specific expression of *BgElo12* and *BgElo24* in *Blattella germanica*. AC: Abdominal cuticle, FB: Fat body, He: Head, Ov: Ovaries, Th: Thorax, Cg: Colleterial gland, Gu: Gut, ED: Ejaculatory duct, MT: Malpighian tubules. Data are shown as mean ± SEM; and each sample was collected from 4 (AC, Th, Gu), 8 (FB, He, Ov, CG, ED), and 12 (MT) cockroaches. Different letters indicate significant differences between groups using Welch's ANOVA (Games-Howell multiple comparisons test, $P < 0.05$), n = 4.

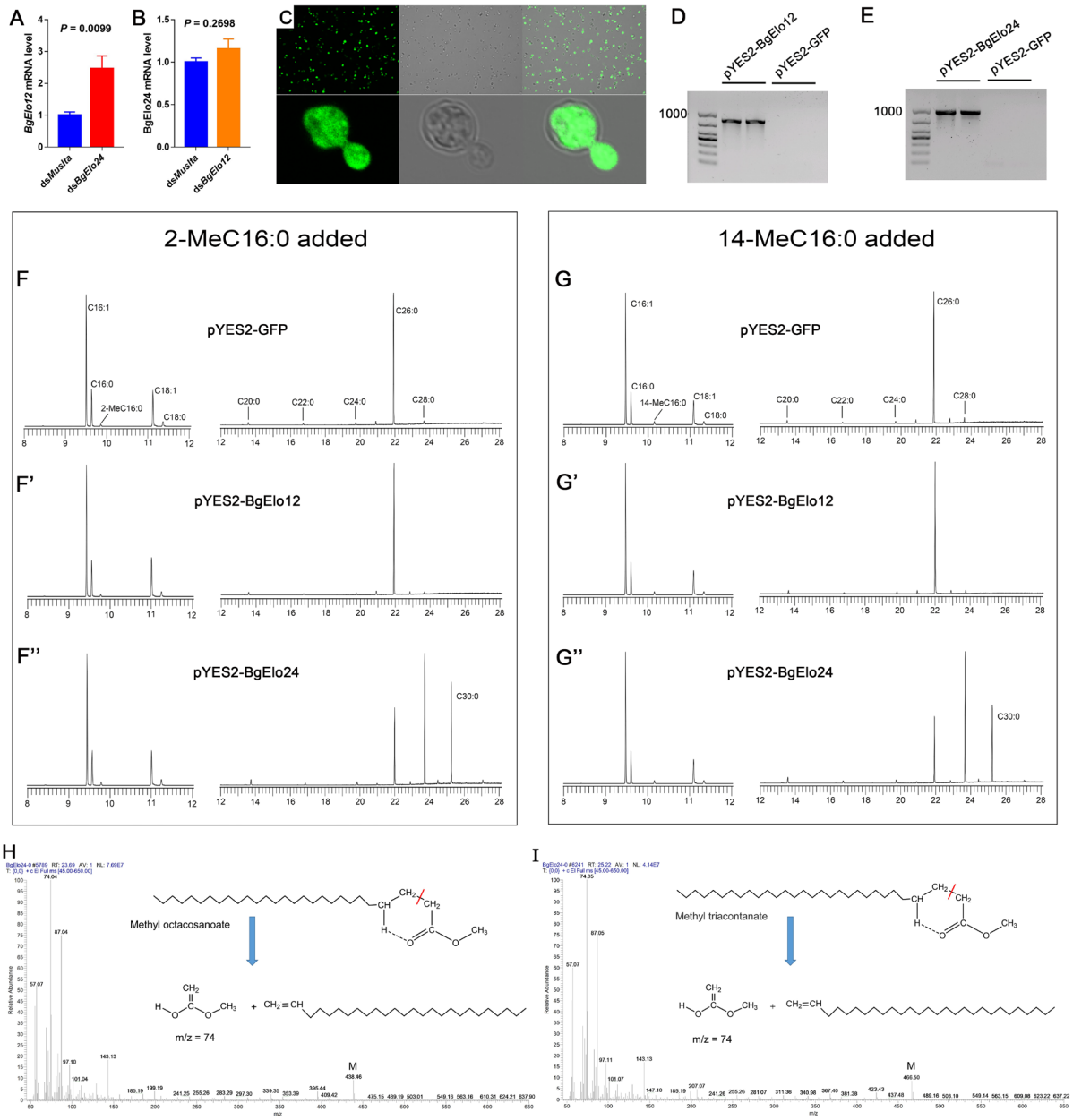

Figure 4–figure supplement 1. Heterologous expression of *BgElo12* and *BgElo24 in Blattella germanica*. RNAi of *BgElo24* upregulated the expression of *BgElo12* **(A)**, while RNAi of *BgElo12* did not affect *BgElo24* transcript level **(B)**. Data are shown as mean ± SEM; *P* values were calculated from 4 samples; each sample contained 2 cockroaches; two-tailed Student's *t*-test. **(C)** Detection of GFP protein in the yeast with pYES2-GFP using a FV3000 confocal fluorescence microscope (Olympus). **(D)** and **(E)** RT-PCR analysis of the *BgElo12* and *BgElo24* mRNA after the induction with galactose. **(F)**, **(F')**, and **(F'')** Gas chromatograms of fatty acid methyl esters after adding 2-MeC16:0 into the medium. **(G)**, **(G')**, and **(G'')** Gas chromatogram of fatty acid methyl esters after adding 14-MeC16:0 into the medium. The compositions with retention times between 12 and 28 min

1070 were magnified about 50 times. **(H)** and **(I)** Mass spectra of methyl octacosanoate and methyl triacontanate, both

1071 of which showed a strong characteristic ion fragment (m/z = 74) and M peak.

1072

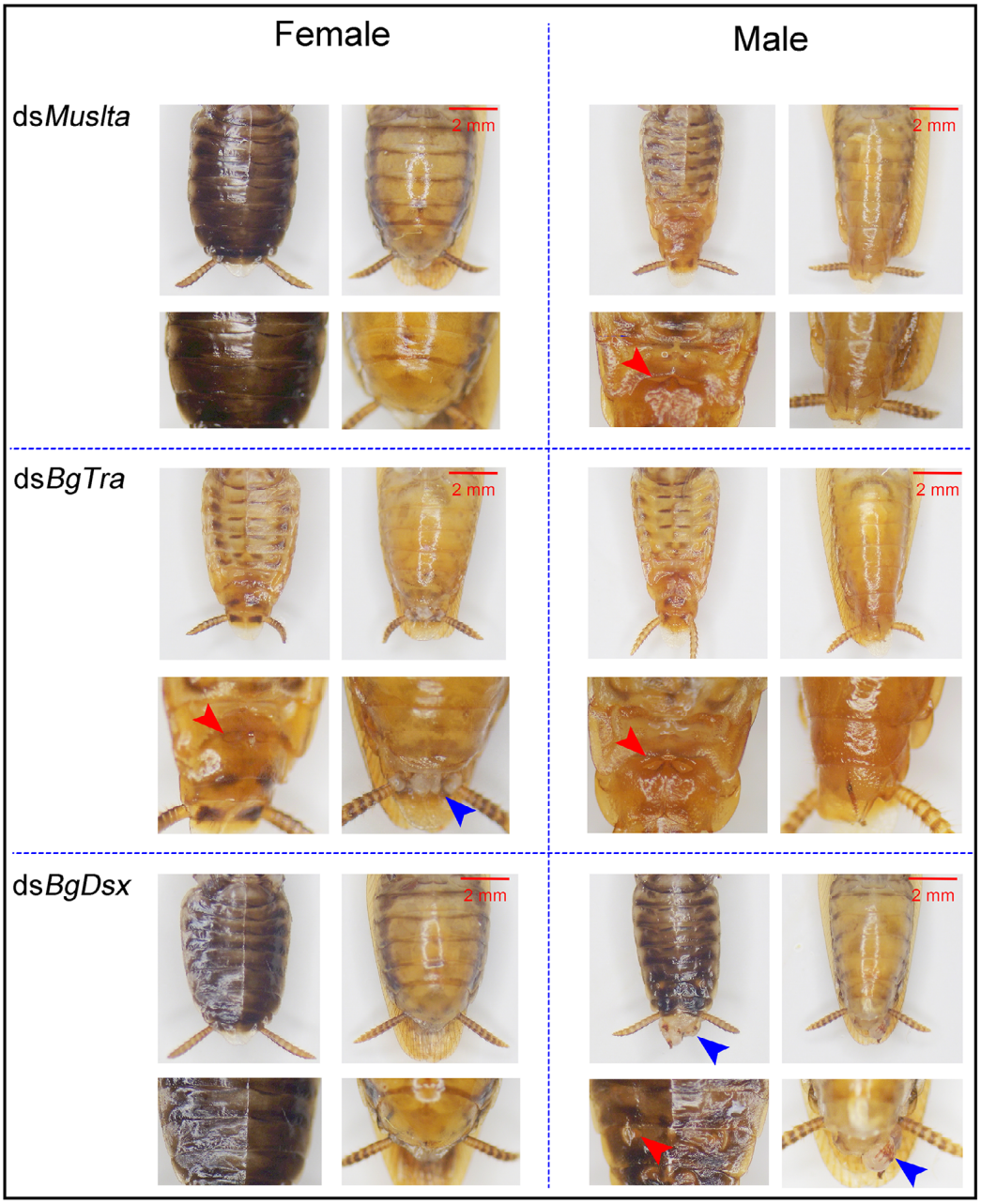

Figure 6–figure supplement 1. The sex-specific developmental functions of *BgTra* and *BgDsx* in *Blattella germanica*. RNAi of *BgTra* in females generated a male-like body size and cuticle color, male-like tergal gland structure and a protruding tissue at the end of the abdomen (left center); RNAi of *BgDsx* in males generated a female-like body color and a protruding tissue at the end of the abdomen, and the partly disappeared tergal gland (right bottom). Other treatments did not generate obvious developmental effects.

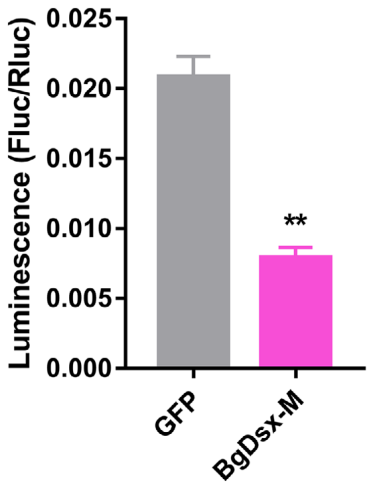

Figure 6-figure supplentment 2. Transcriptional activity of *BgDsx*^{M} on the upstream regulatory sequence of *BgElo12*. Data are shown as mean ± SEM; *P* values were calculated from 12 replicates; two-tailed Student's *t*-test.

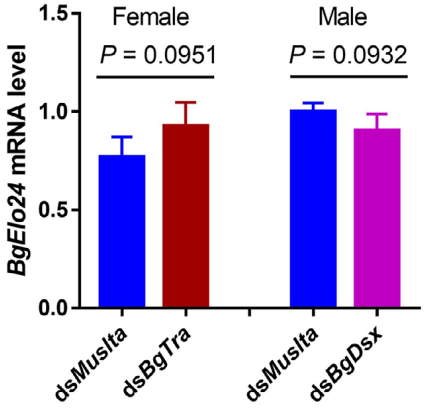

Figure 6–figure supplement 3. Effects of *BgDsx*-RNAi in males and *BgTra*-RNAi in females on *BgElo24* expression. Data are shown as mean ± SEM; *P* values were calculated from 4 replicates (2 cockroaches/replicate); two-tailed Student's *t*-test.

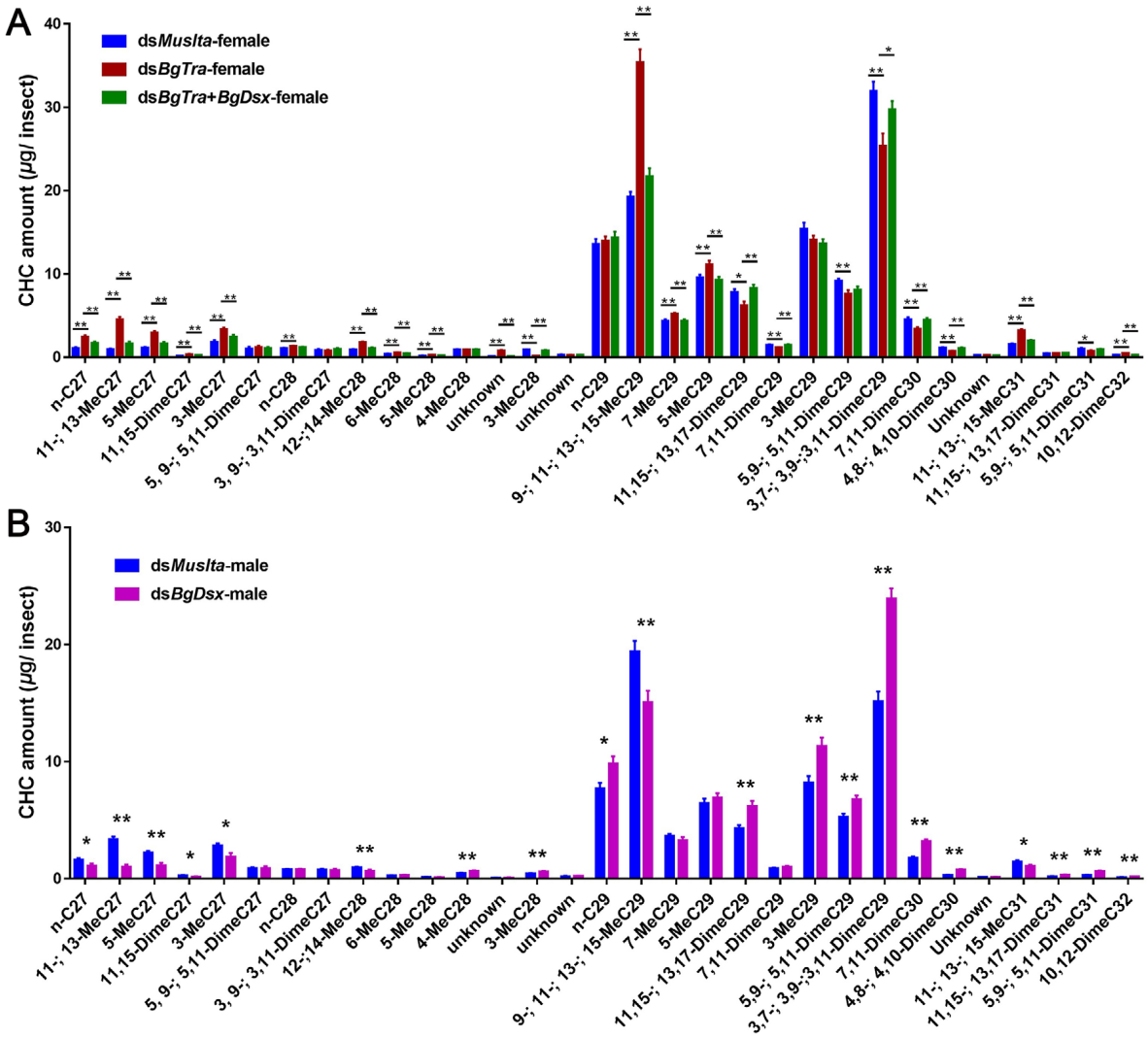

Figure 6–figure supplement 4. Regulation of cuticular hrdrocarbon profiles by sex-differentiation genes. Data are shown as mean ± SEM, *$P < 0.05$, **$P < 0.01$, two-tailed Student's *t*-test, n = 14 (ds*Muslta*-female), 12 (ds*BgTra*-female), 14 (ds*BgTra*+ds*BgDsx*-female), 12 (ds*Muslta*-male), and 16 (ds*BgDsx*-male).

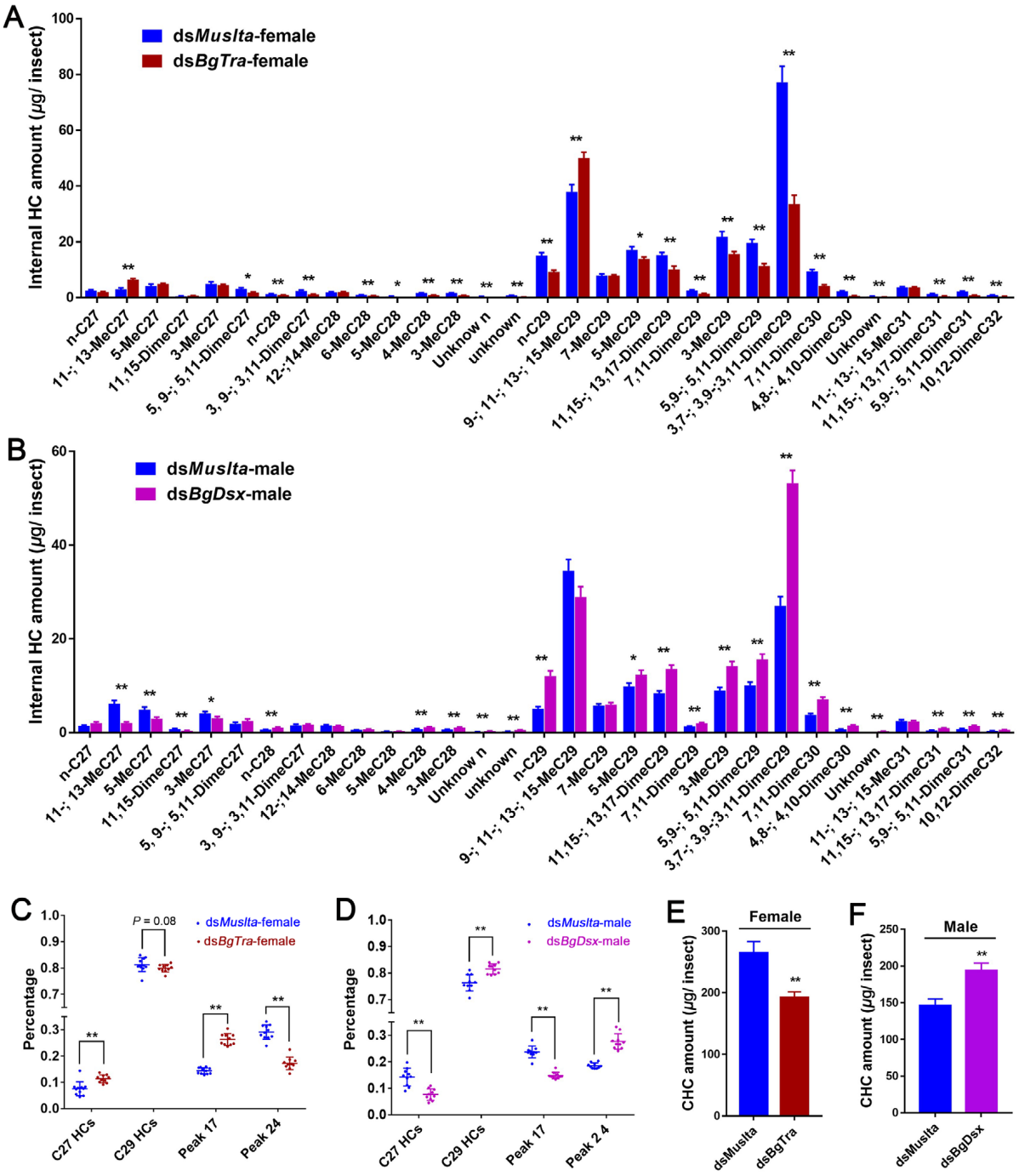

Figure 6–figure supplement 5. Regulation of internal hrdrocarbon profiles by sex-differentiation genes. **(A)** and **(B)** Effects of *BgTra*-RNAi in females and *BgDsx*-RNAi in males on sex-specific internal hydrocarbon profiles. **(C)** and **(D)** Proportion changes of representative internal hydrocarbons after RNAi of *BgTra* in females and *BgDsx* in males. **(E)** and **(F)** Effects of *BgTra*-RNAi in females and *BgDsx*-RNAi in males on total amounts of internal hydrocarbons. Data are shown as mean ± SEM, $*P < 0.05$, $**P < 0.01$, two-tailed Student's *t*-test, n = 10 or 11.

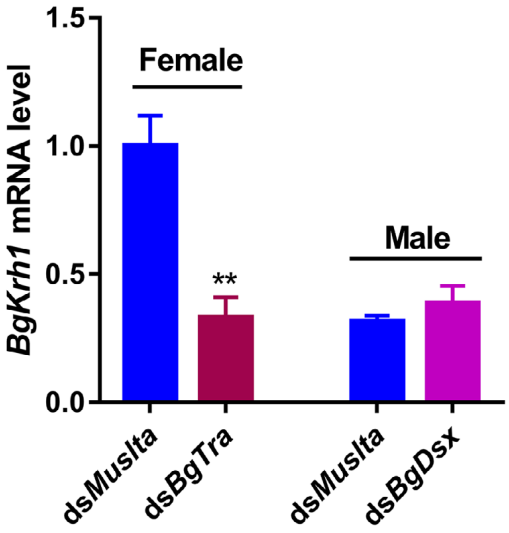

Figure 6–figure supplement 6. Regulation of *BgKrh1* by *BgTra* in females. Data are shown as mean ± SEM, *P* values were calculated from 4 replicates (2 cockroaches/replicate), $^{**}P < 0.01$, two-tailed Student's *t*-test.